

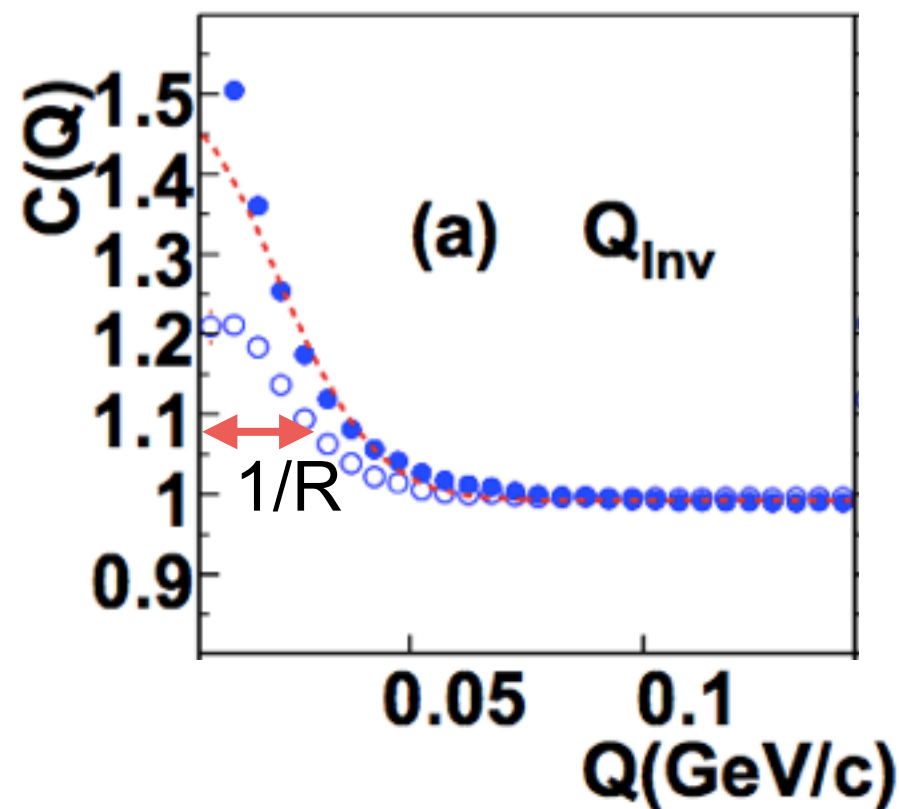
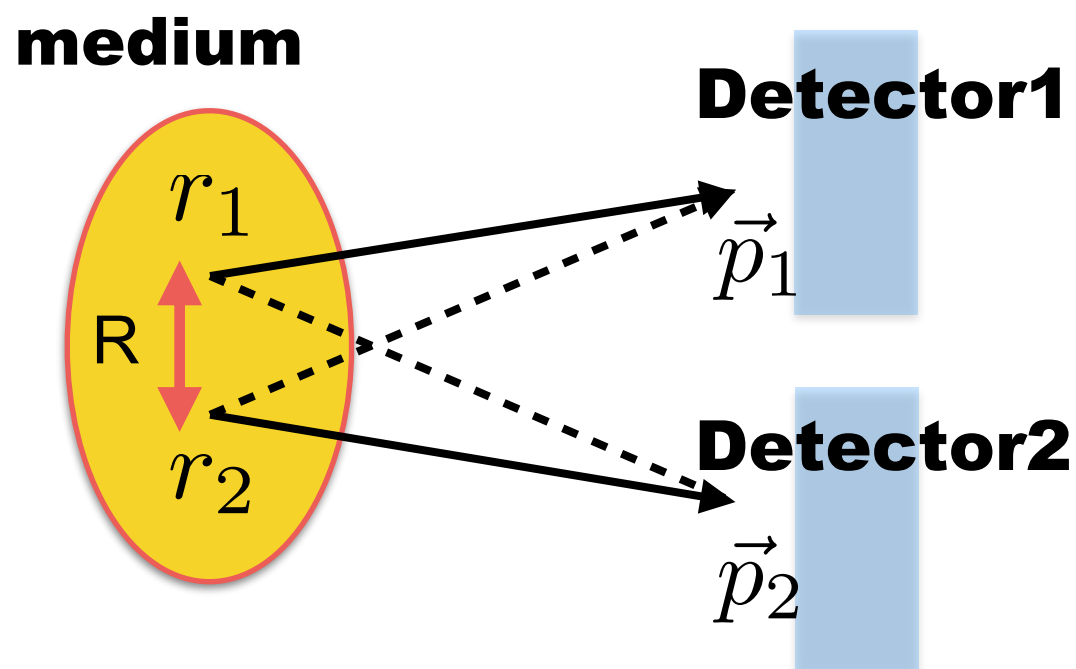


***Azimuthal-angle dependence of pion femtoscopy
relative to the first-order event plane
in $\sqrt{s_{NN}} = 200$ GeV Au+Au and Cu+Au collisions at
STAR***

Yota Kawamura
for the STAR Collaboration
January 10th, 2019
WWND2019 @ Beaver Creek



- HBT can scope **the source size at kinetic freeze-out**
- ✓ Measure quantum interference between two identical particles



STAR Collaboration, Phys. Rev. Lett. 87 (2001) 82301

Theory

$$C_2 = \frac{P(p_1, p_2)}{P(p_1)P(p_2)} \approx 1 + \exp(-R^2 Q_{inv}^2)$$

$$\vec{q} = \vec{p}_2 - \vec{p}_1 \quad Q_{inv} = \sqrt{q_x^2 + q_y^2 + q_z^2 - q_0^2}$$

Experimentally

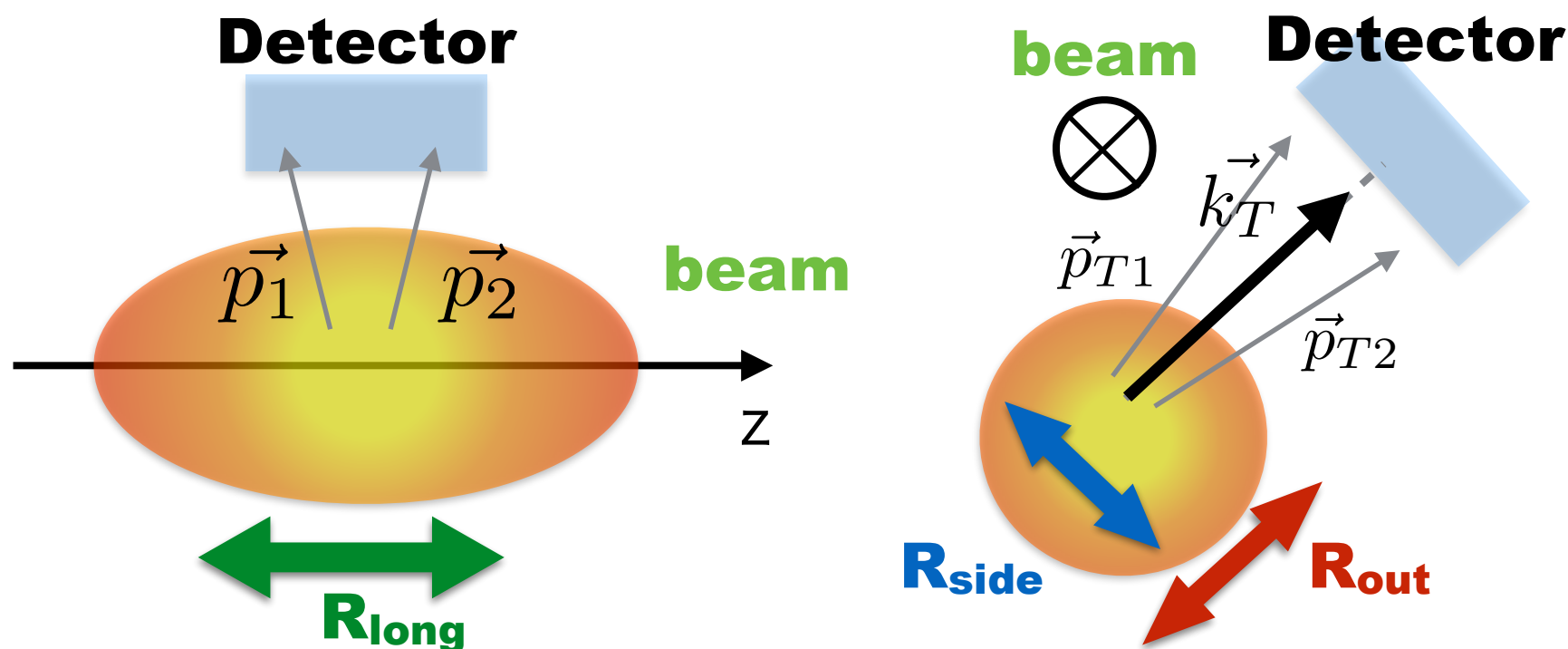
$$C(q) = \frac{N(q)}{D(q)} \quad \bullet \text{ Event mixing}$$

N: pair distribution in same event (real)

D: pair distribution from different events (mixed)

- Make correlation function as a function of relative momentum (q)
- One can extract the source radius by fitting with theoretical formula

- **Bertsch-Pratt Parameterization** (S. Pratt, Phys. Rev. D 33, (1986) 72 , G. Bertsch et al., Phys. Rev. C 37, (1988) 1896)



$$\vec{k}_T = \frac{1}{2}(\vec{p}_{T1} + \vec{p}_{T2})$$

$$\vec{q}_{out} \parallel \vec{k}_T$$

$$\vec{q}_{side} \perp \vec{k}_T$$

- 3-dimensional radii use

✓ **R_{long}** : Source size parallel to the beam direction

✓ **R_{out}** : Source size parallel to the pair transverse momentum (k_T) + emission duration

✓ **R_{side}** : Source size perpendicular to **R_{out}** and **R_{long}**

✓ **Fit function:**

$$C(\vec{q}) = N[(1 - \lambda) + \lambda K(\vec{q})(1 + G(\vec{q}))]$$

$$G(\vec{q}) = \exp(-R_{out}^2 q_{out}^2 - R_{side}^2 q_{side}^2 - R_{long}^2 q_{long}^2)$$

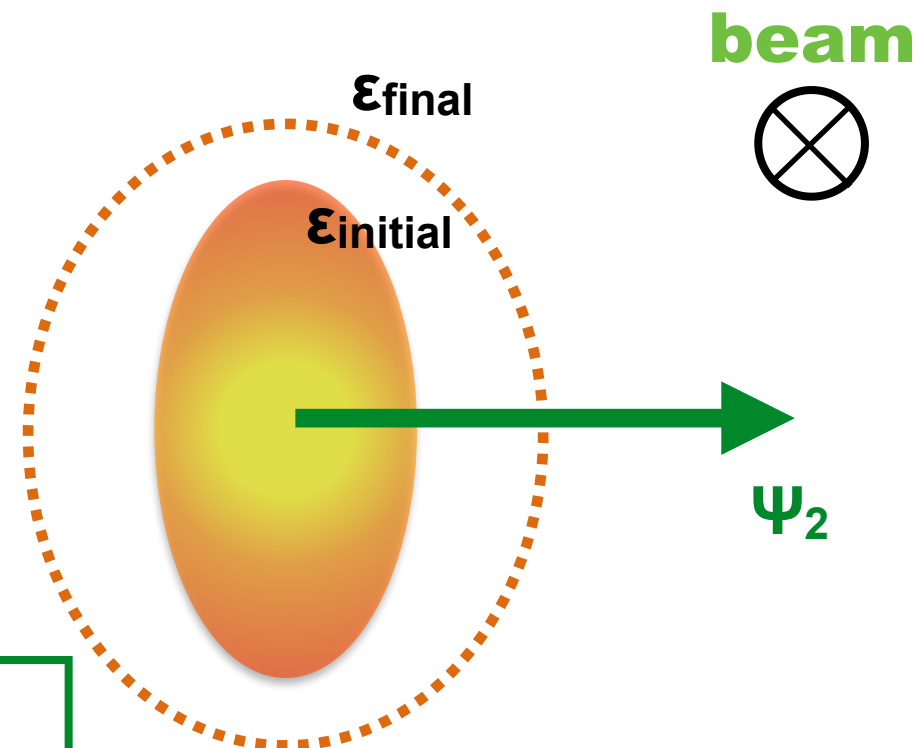
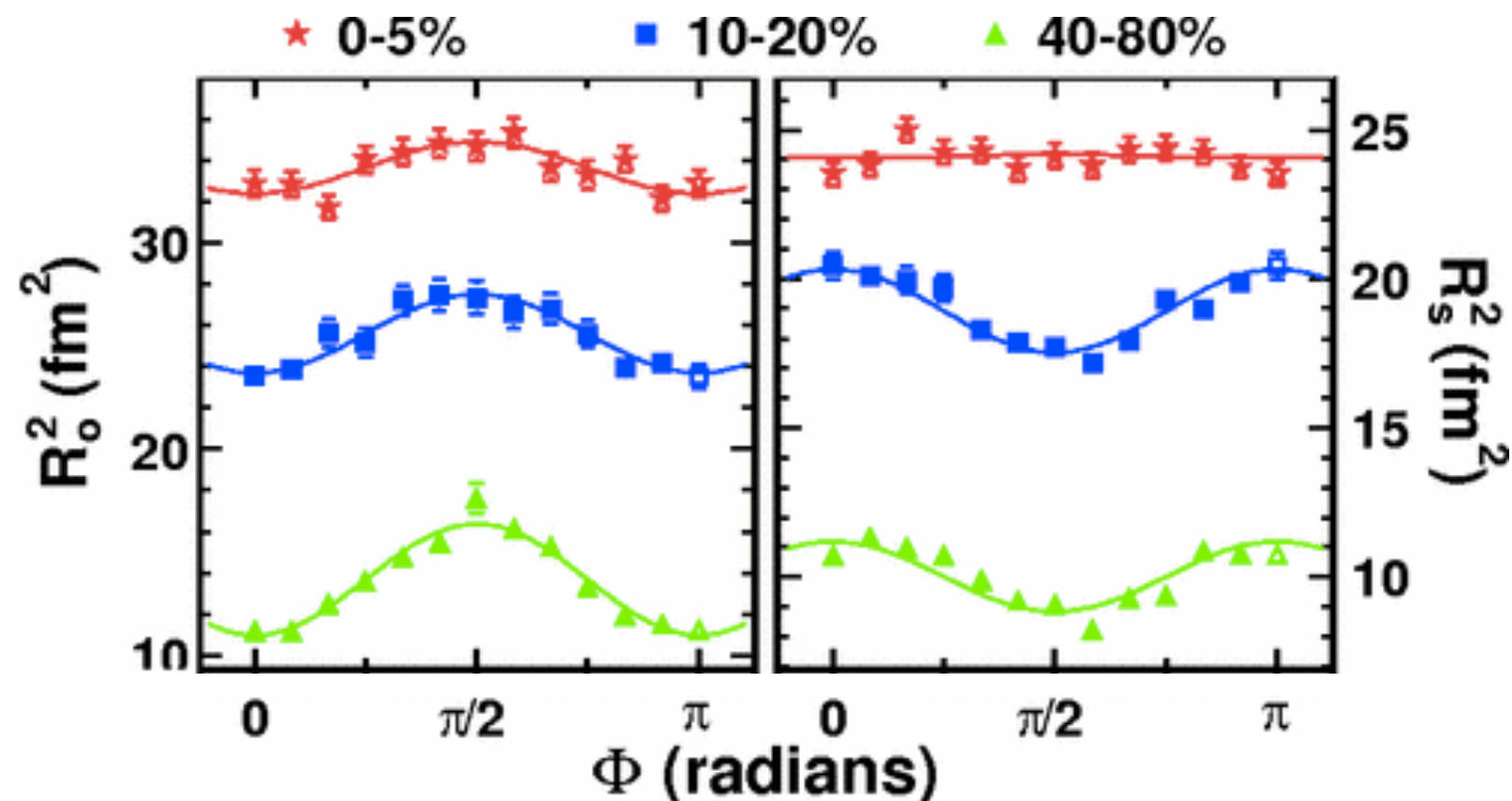
N : Normalization , **K(q)** : Coulomb correction, **λ** : Correlation strength

✓ Pair relative momentum \vec{q} is decomposed into three projection

{**q_{out}**, **q_{side}** and **q_{long}**}

✓ Extract radii from fit of correlation function

STAR collaboration, Phys. Rev. Lett. 93, (2004) 012301



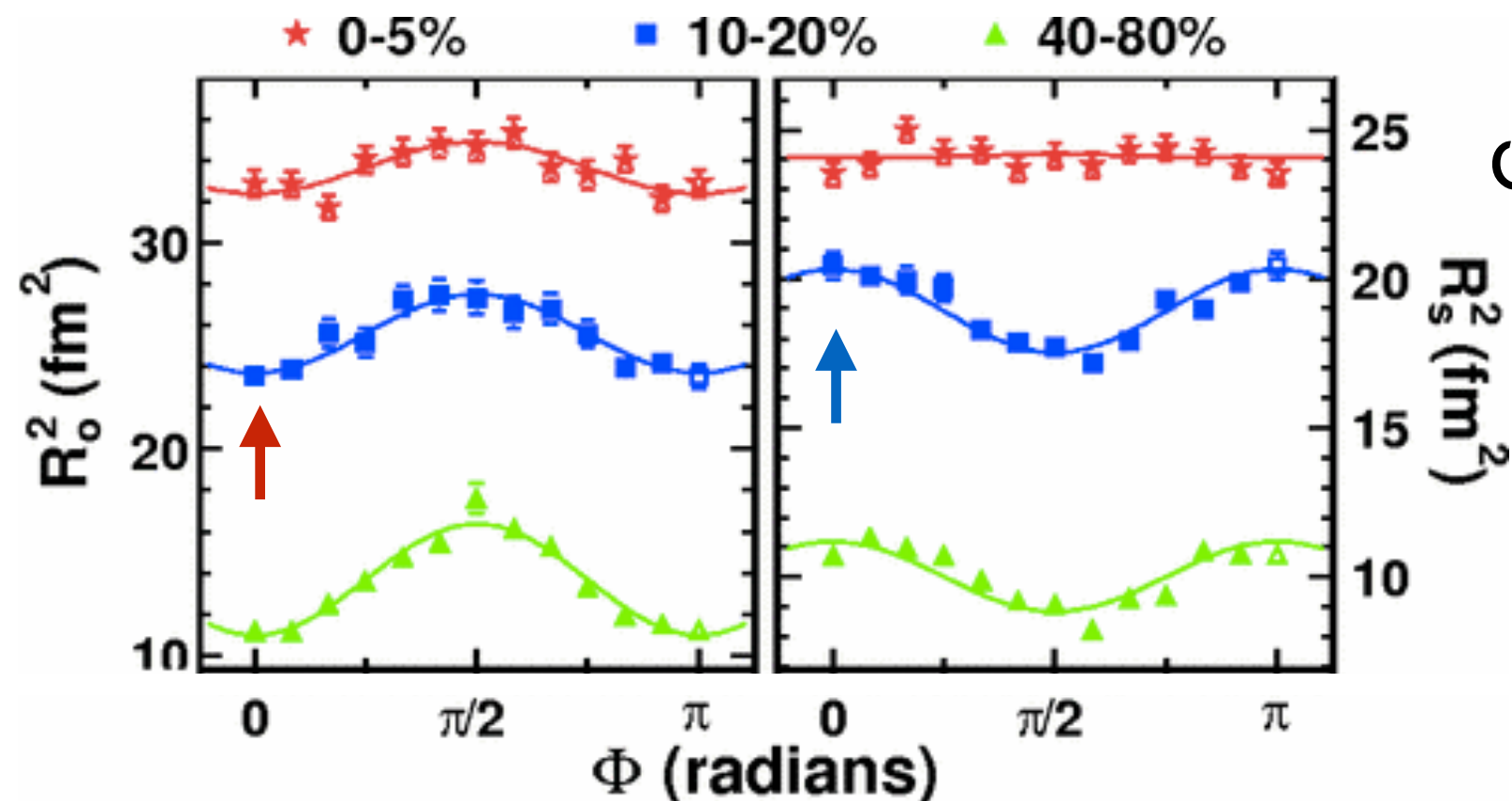
$$\epsilon_{\text{final}} \approx 2 \frac{R_{s,2}^2}{R_{s,0}^2}$$

$R_{\mu,0}^2$: Average radius
 $R_{\mu,2}^2$: 2nd-order oscillation magnitude

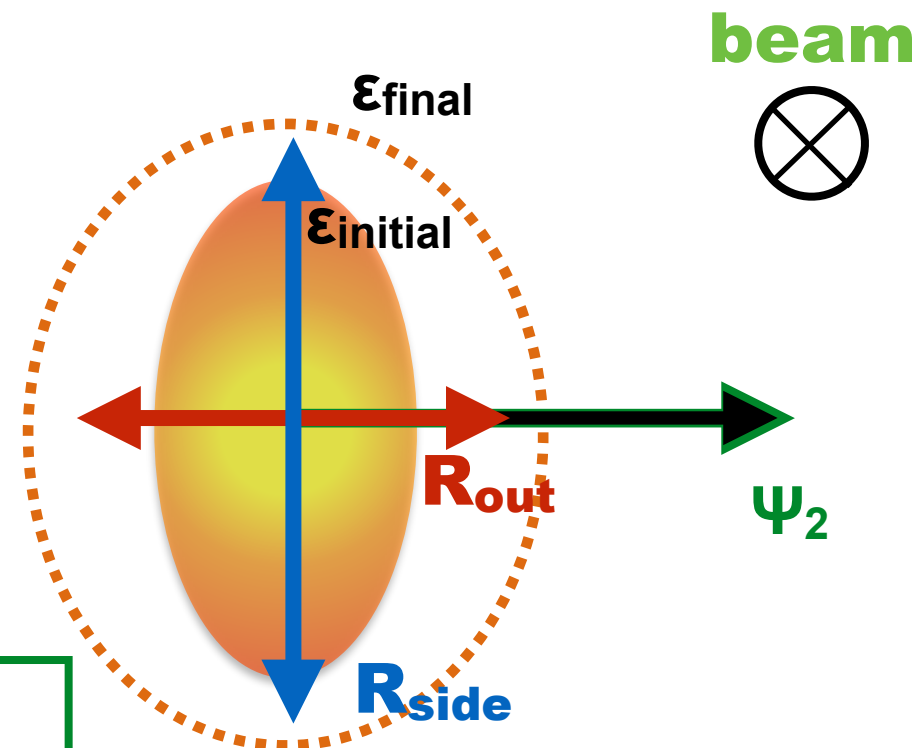
- Fit function:
 $R_{\mu,0}^2 + 2 R_{\mu,2}^2 \cos(2(\phi - \Psi_{\text{RP}}))$, ($\mu = \text{out, side}$)

- Final eccentricity can be measured by HBT radii w.r.t. Ψ_2
- $\phi = 0^\circ$ R_{out} : short axis of ellipse, R_{side} : long axis of ellipse
- $\phi = 90^\circ$ R_{out} : long axis of ellipse, R_{side} : short axis of ellipse
- Out-of-plane expanded final source ($\epsilon_{\text{final}} > 0$) can be measured
- It depends on initial eccentricity, source evolution, etc

STAR collaboration, Phys. Rev. Lett. 93, (2004) 012301



$\varphi_{\text{pair}} = 0^\circ$

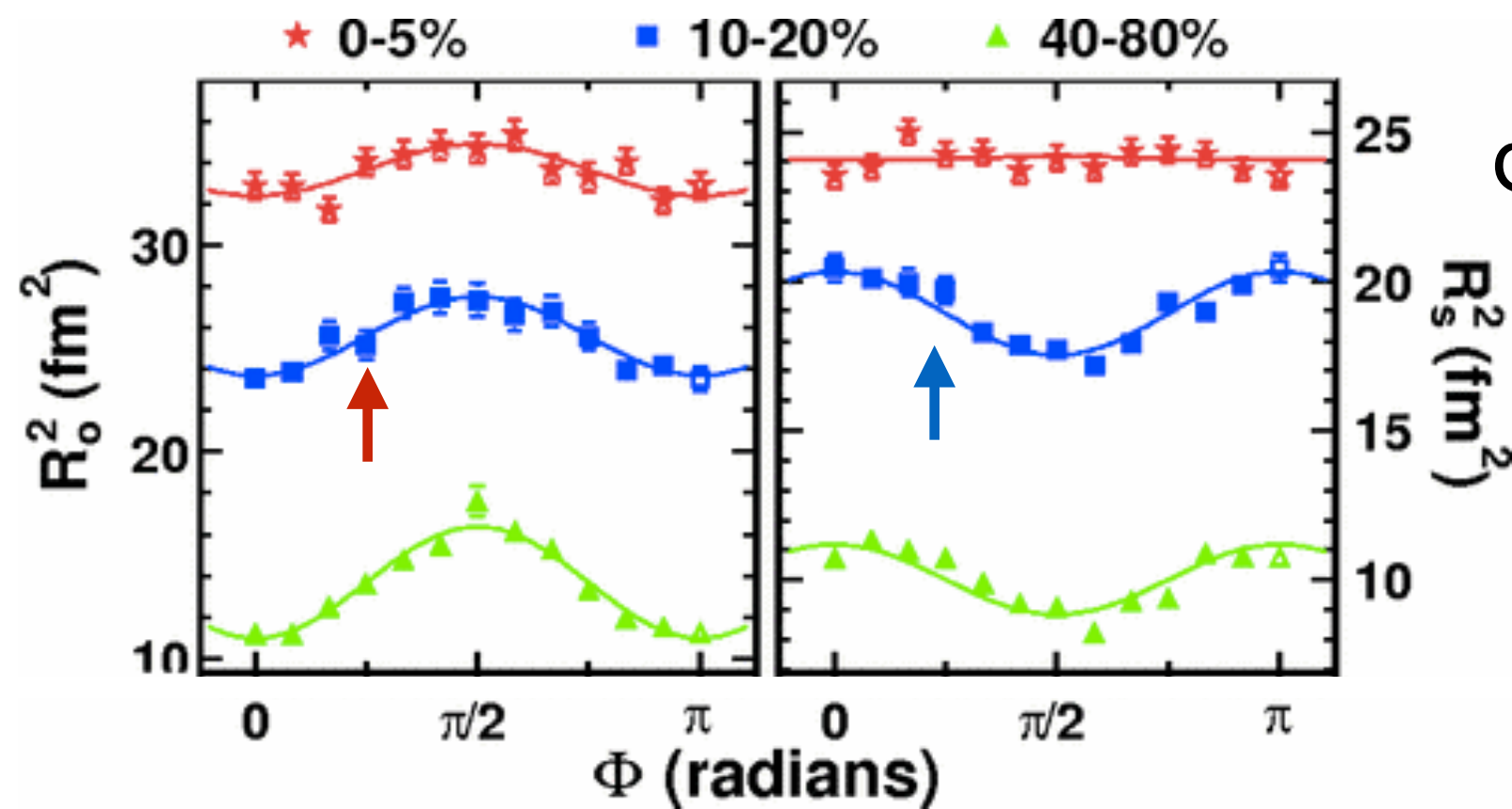


$\epsilon_{\text{final}} \approx 2 \frac{R_{s,2}^2}{R_{s,0}^2}$ $R_{\mu,0}^2$: Average radius
 $R_{\mu,2}^2$: 2nd-order oscillation magnitude

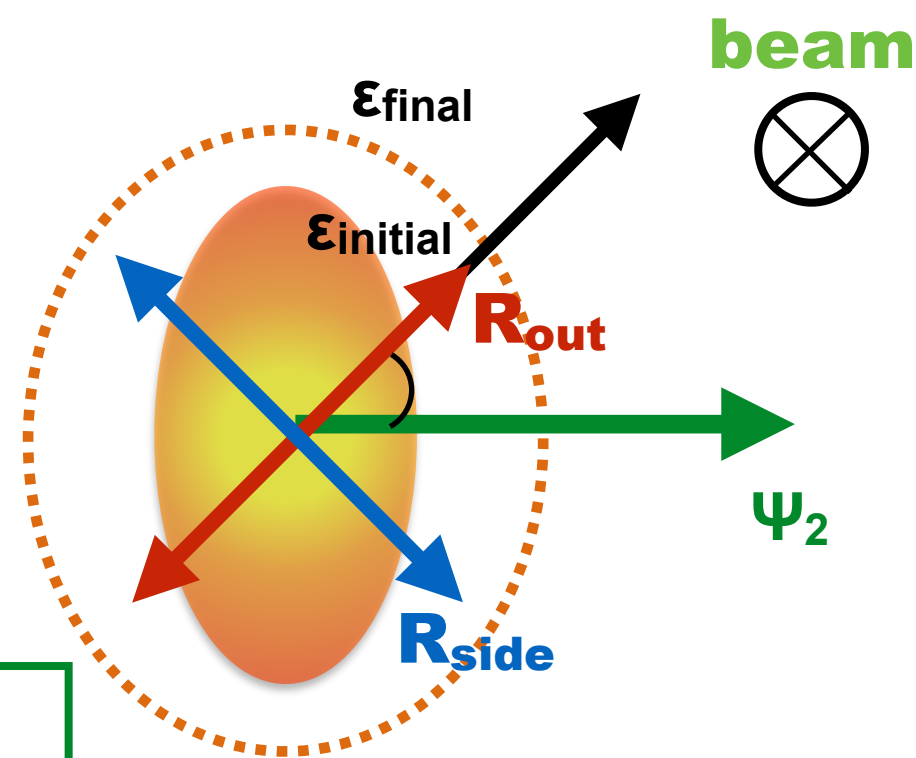
- Fit function:
 $R_{\mu,0}^2 + 2 R_{\mu,2}^2 \cos(2(\varphi - \Psi_{\text{RP}}))$, ($\mu = \text{out, side}$)

- Final eccentricity can be measured by HBT radii w.r.t. Ψ_2
- $\varphi = 0^\circ$ R_{out} : short axis of ellipse, R_{side} : long axis of ellipse
- $\varphi = 90^\circ$ R_{out} : long axis of ellipse, R_{side} : short axis of ellipse
- Out-of-plane expanded final source ($\epsilon_{\text{final}} > 0$) can be measured
- It depends on initial eccentricity, source evolution, etc

STAR collaboration, Phys. Rev. Lett. 93, (2004) 012301



$$\varphi_{\text{pair}} = 45^\circ$$

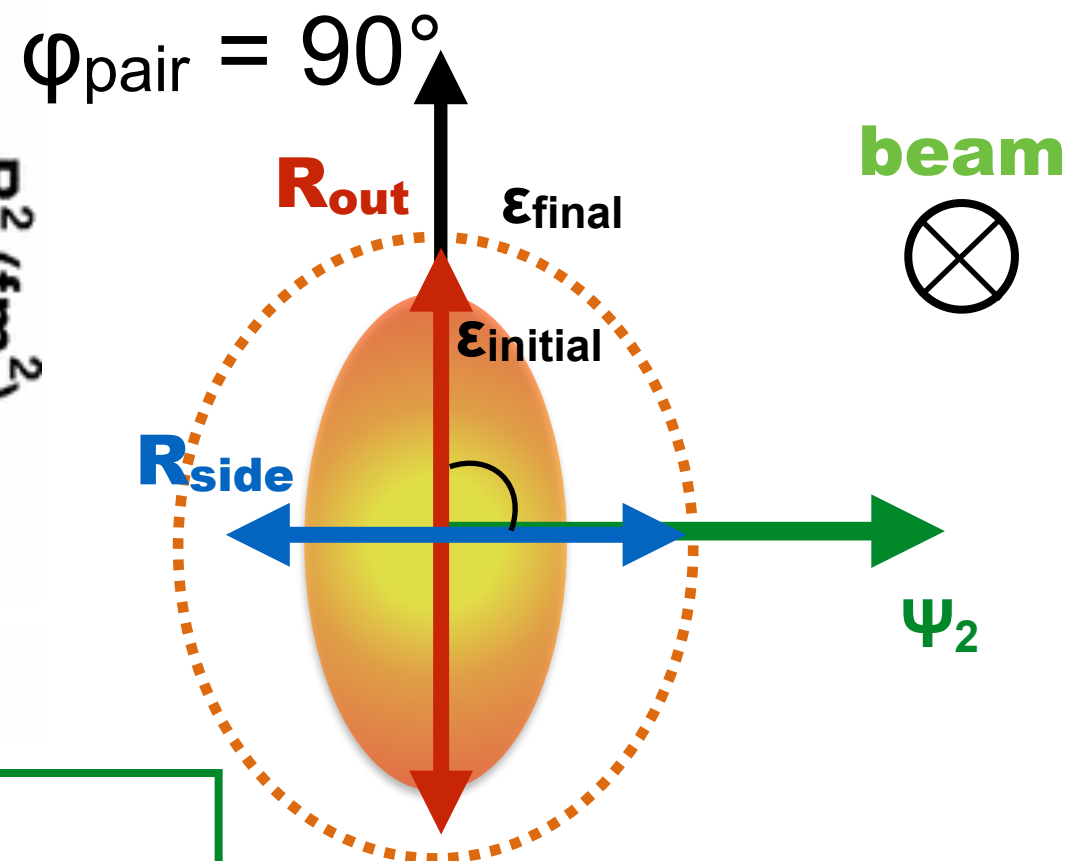
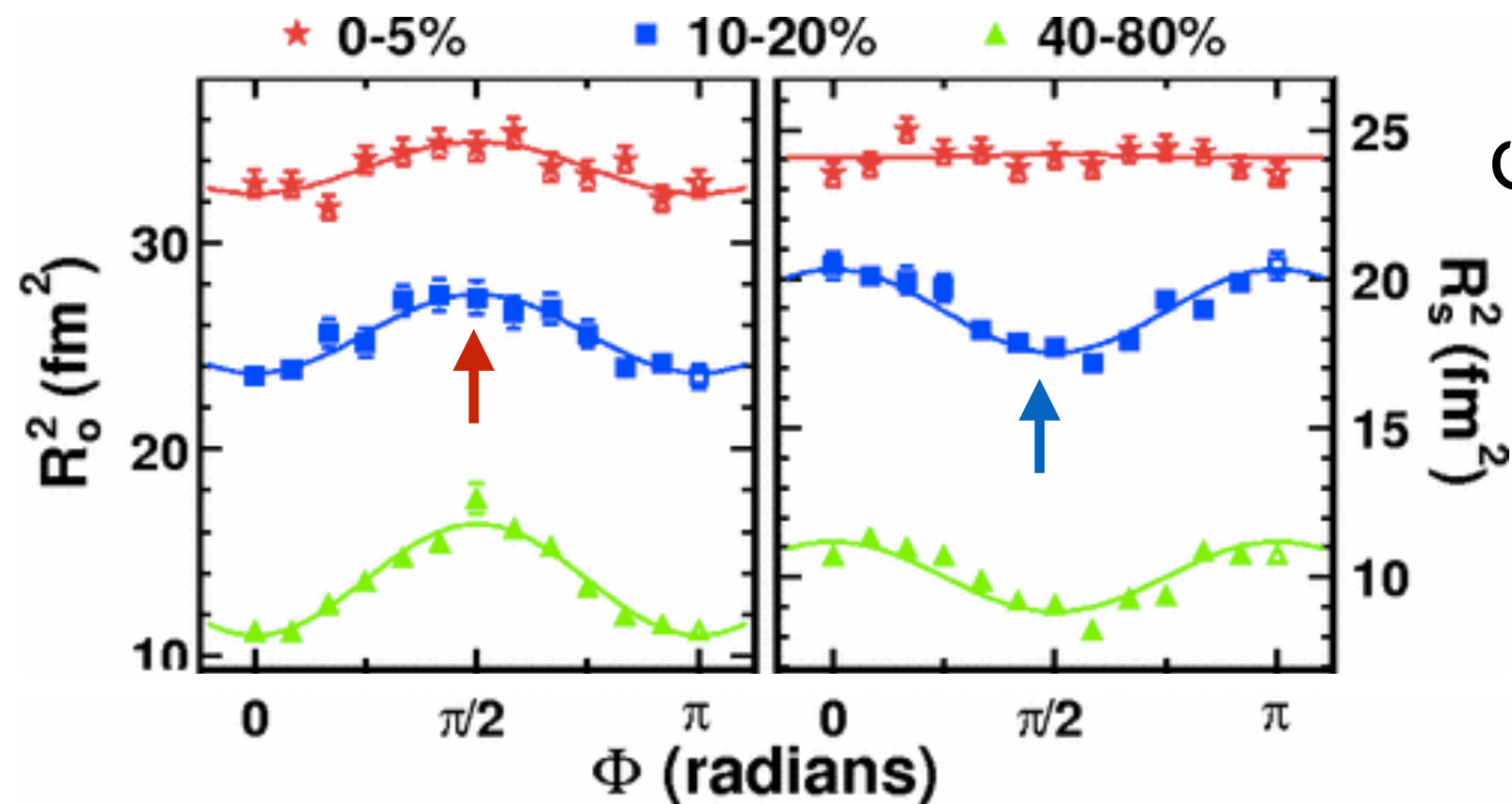


$\epsilon_{\text{final}} \approx 2 \frac{R_{s,2}^2}{R_{s,0}^2}$ $R_{\mu,0}^2$: Average radius
 $R_{\mu,2}^2$: 2nd-order oscillation magnitude

- Fit function:
 $R_{\mu,0}^2 + 2 R_{\mu,2}^2 \cos(2(\varphi - \Psi_{\text{RP}}))$, ($\mu = \text{out, side}$)

- Final eccentricity can be measured by HBT radii w.r.t. Ψ_2
- $\varphi = 0^\circ$ R_{out} : short axis of ellipse, R_{side} : long axis of ellipse
- $\varphi = 90^\circ$ R_{out} : long axis of ellipse, R_{side} : short axis of ellipse
- Out-of-plane expanded final source ($\epsilon_{\text{final}} > 0$) can be measured
- It depends on initial eccentricity, source evolution, etc

STAR collaboration, Phys. Rev. Lett. 93, (2004) 012301



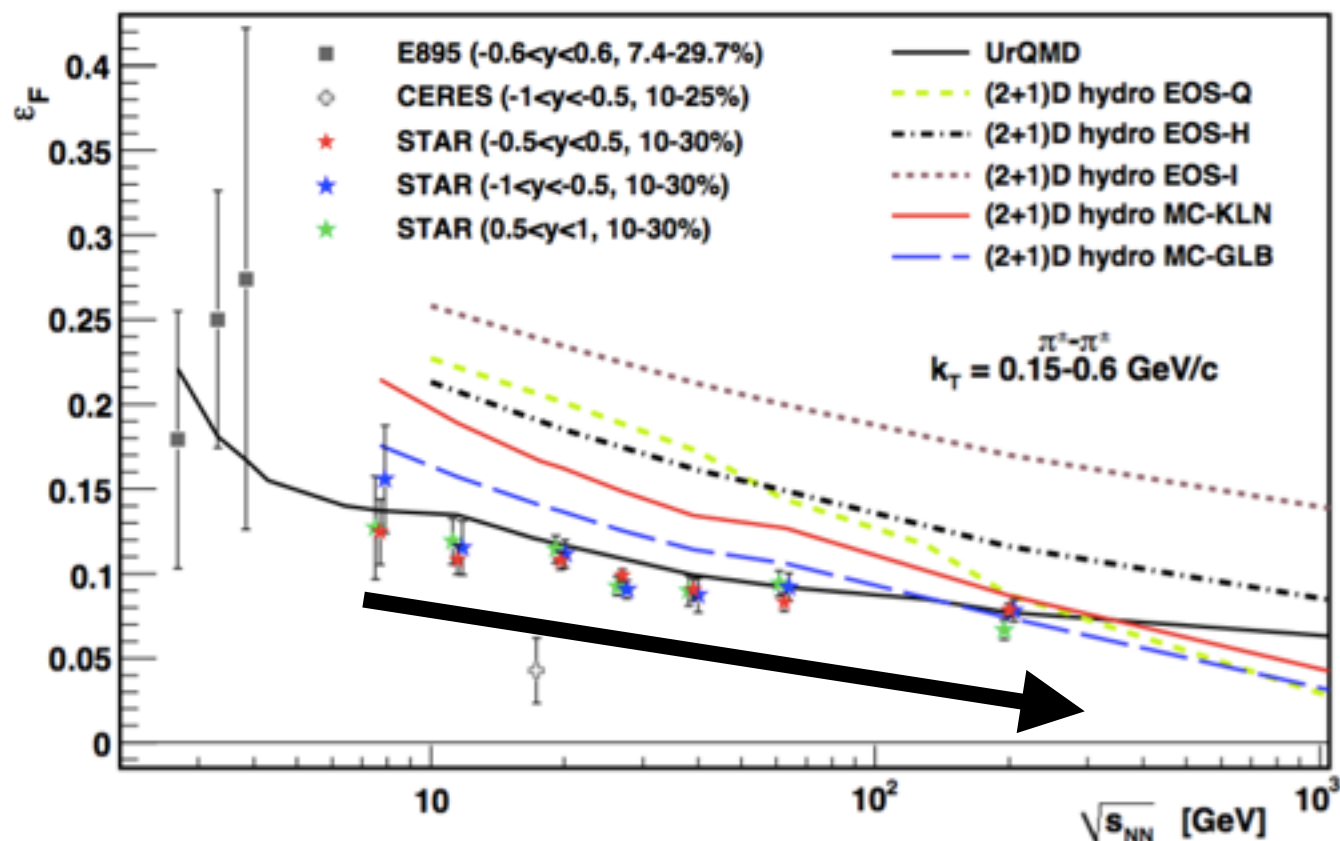
$$\epsilon_{\text{final}} \approx 2 \frac{R_{s,2}^2}{R_{s,0}^2}$$

$R_{\mu,0}^2$: Average radius
 $R_{\mu,2}^2$: 2nd-order oscillation magnitude

- Fit function:
 $R_{\mu,0}^2 + 2 R_{\mu,2}^2 \cos(2(\phi - \Psi_{\text{RP}}))$, ($\mu = \text{out, side}$)

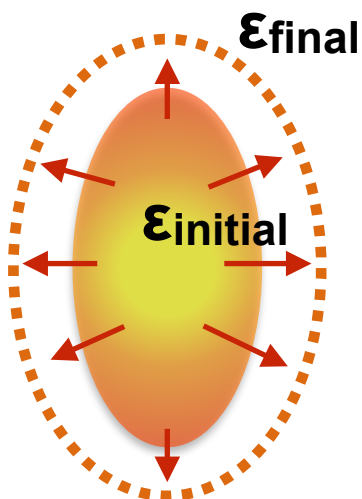
- Final eccentricity can be measured by HBT radii w.r.t. Ψ_2
- $\phi = 0^\circ$ R_{out} : short axis of ellipse, R_{side} : long axis of ellipse
- $\phi = 90^\circ$ R_{out} : long axis of ellipse, R_{side} : short axis of ellipse
- Out-of-plane expanded final source ($\epsilon_{\text{final}} > 0$) can be measured
- It depends on initial eccentricity, source evolution, etc

- Final eccentricity via HBT

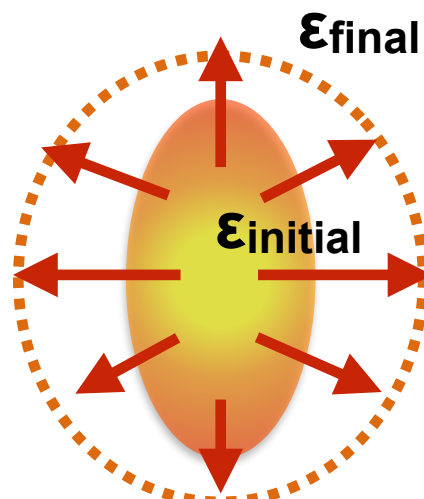


STAR Collaboration, Phys. Rev. C 92 (2015) 014904

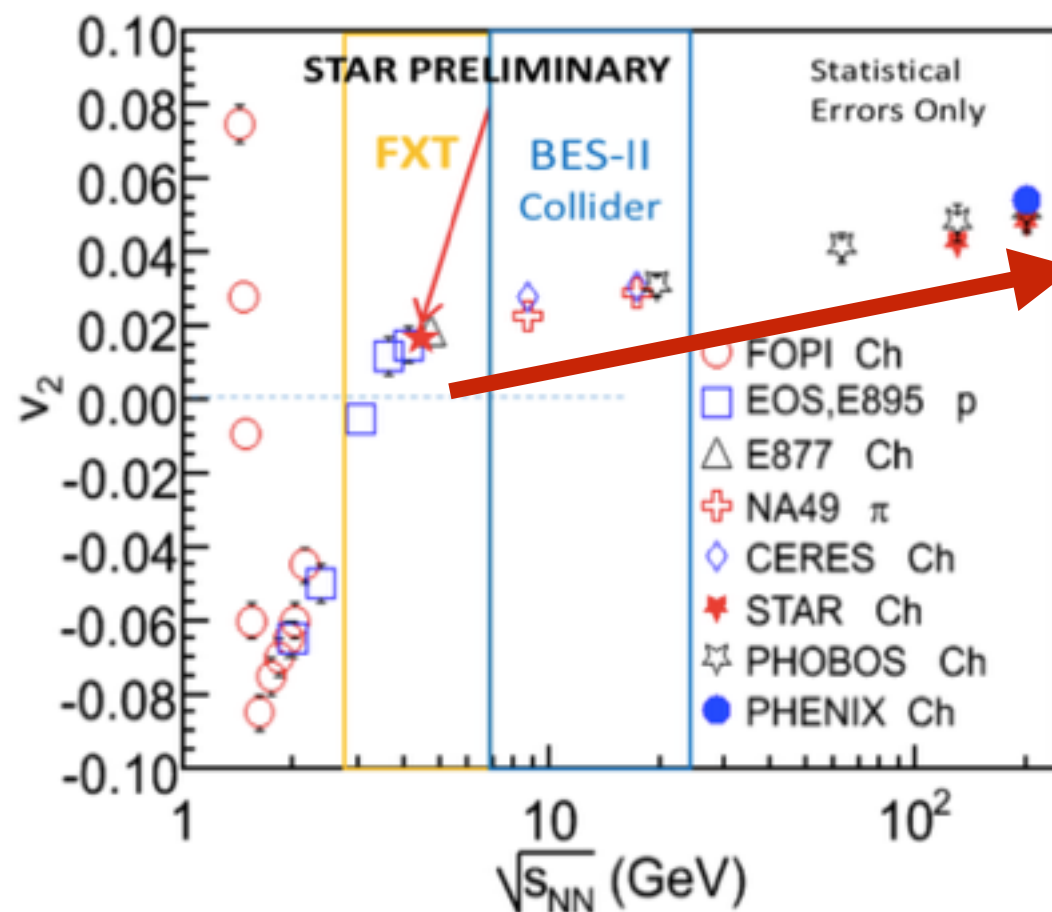
✓ Low energy



✓ High energy



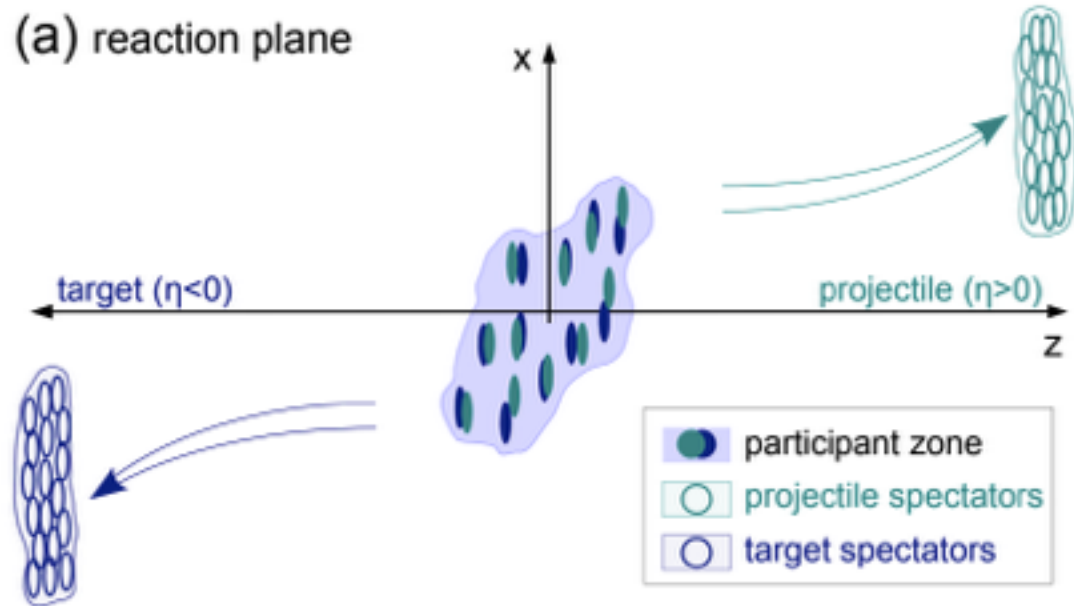
- Momentum space anisotropy



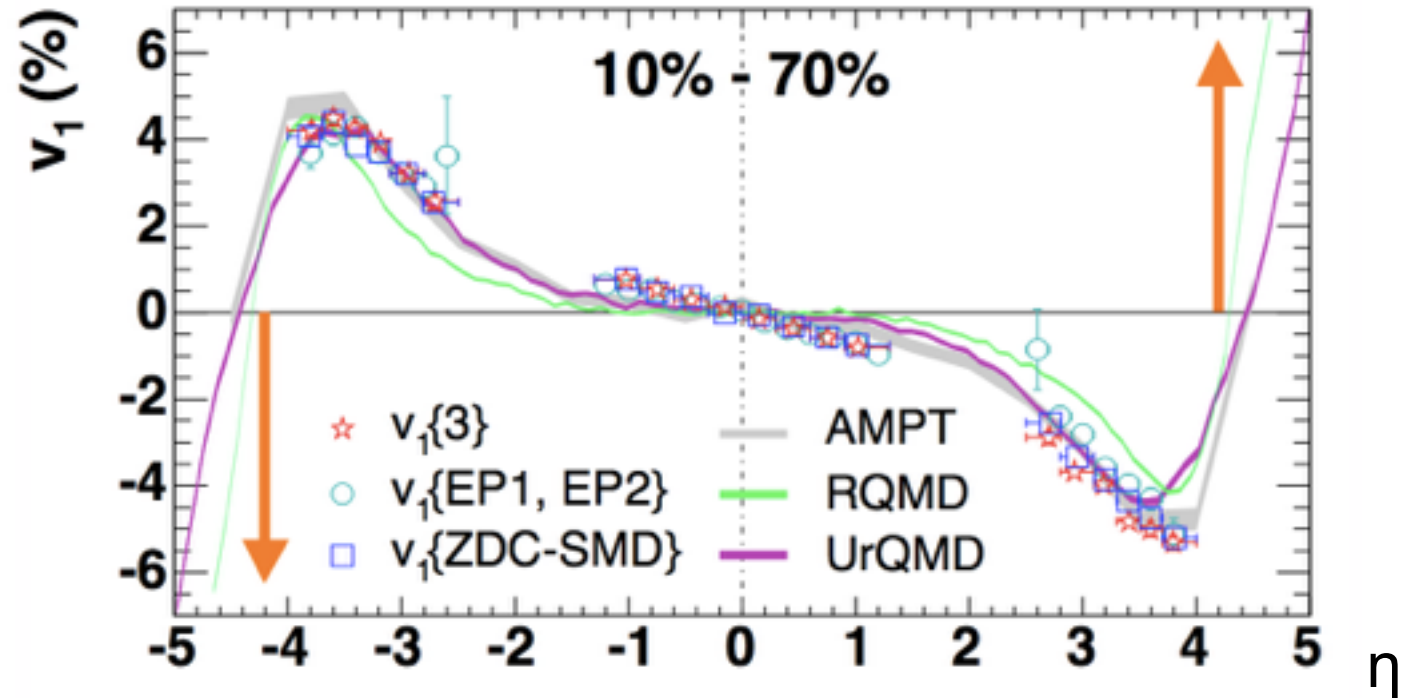
STAR, Quark Matter 2018

• Final eccentricity decreases (more round shape) with increasing collision energy due to longer lifetime and stronger pressure gradients

ALICE Collaboration, Phys. Rev. Lett. 111 (2013) 232302



STAR Collaboration, Phys. Rev. C 73 (2006) 34903



Au+Au 62.4 GeV, Charged particle v_1

→ The direction of flow for spectator neutrons (measured in ZDC).

✓ Directed flow is generated by the interaction between spectator and participant particles

✓ Quantified by the 1st harmonic in the Fourier expansion as v_1

$$v_1 = \langle \cos(\phi - \Psi_1) \rangle$$

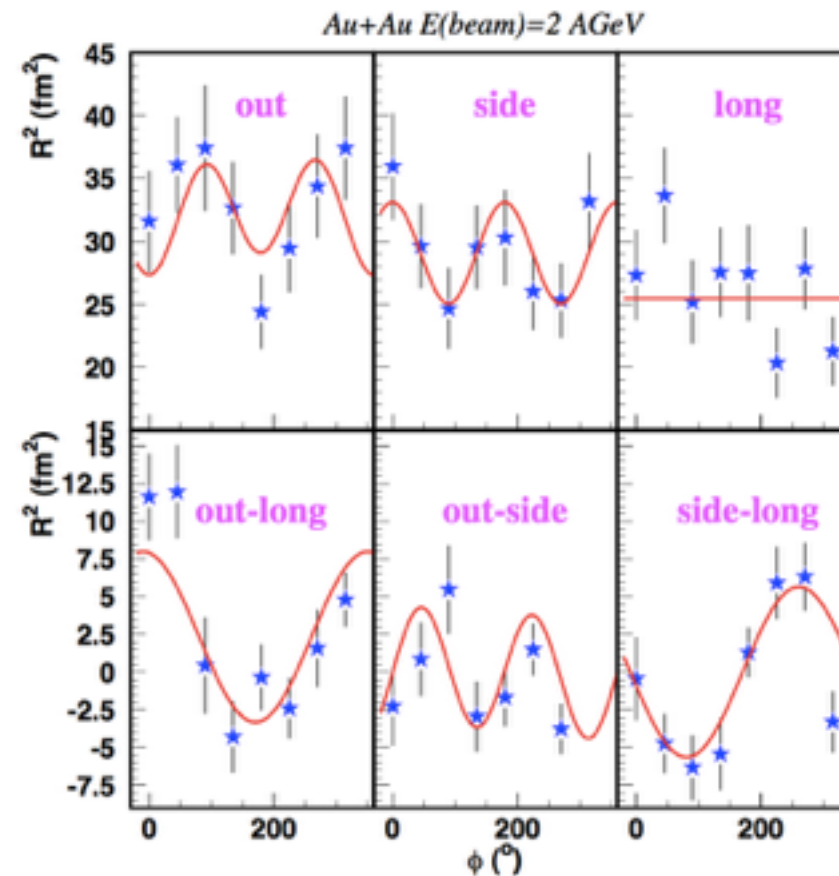
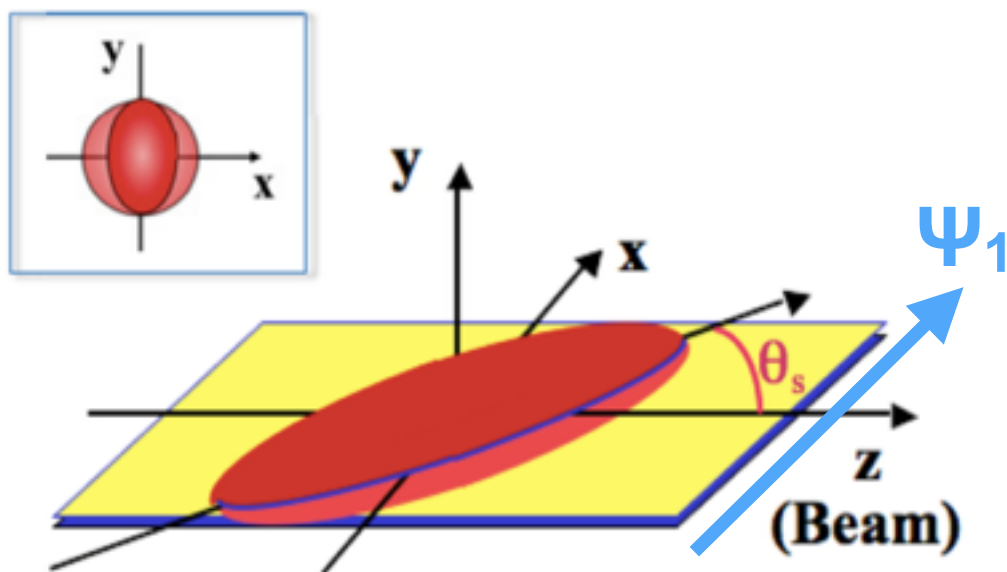
✓ $v_1(\eta)$ is crossing zero 3 times at around midrapidity, forward and backward rapidities
 -> “wiggly structure”

✓ Possible signature of phase transition

J. Brachmann et al. Phys. Rev. C 61 (2000) 024909

✓ Hydrodynamic models cannot explain only v_1 (unlike to v_2 or v_3)

M. A. Lisa et al. New J. Phys. 13 (2011) 065006



- v_1 signal can be generated from assuming the “tilted” source initial conditions
- HBT measurement w.r.t. Ψ_1 can scope source tilt at freeze-out by including cross terms in the fit function

✓ Fit function with cross terms:

$$C(\vec{q}) = N[(1 - \lambda) + \lambda K(\vec{q})(1 + G(\vec{q}))]$$

$$G(\vec{q}) = \exp(-R_{out}^2 q_{out}^2 - R_{side}^2 q_{side}^2 - R_{long}^2 q_{long}^2 - 2R_{os}^2 q_{out} q_{side} - 2R_{ol}^2 q_{out} q_{long} - 2R_{sl}^2 q_{side} q_{long})$$

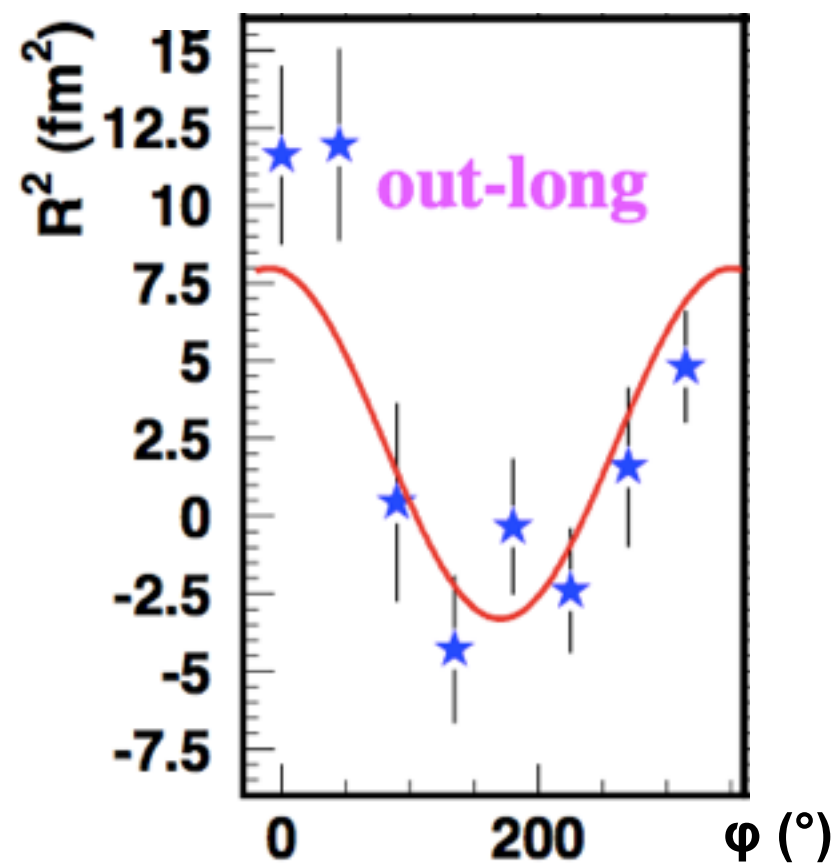
- **Important parameters: R_{ol} , R_{sl}**
- **If final source is tilted, R_{ol} and R_{sl} cross terms will have oscillation w.r.t. Ψ_1**

- 3D



:Out - Long plane

- Projection Out - Long plane



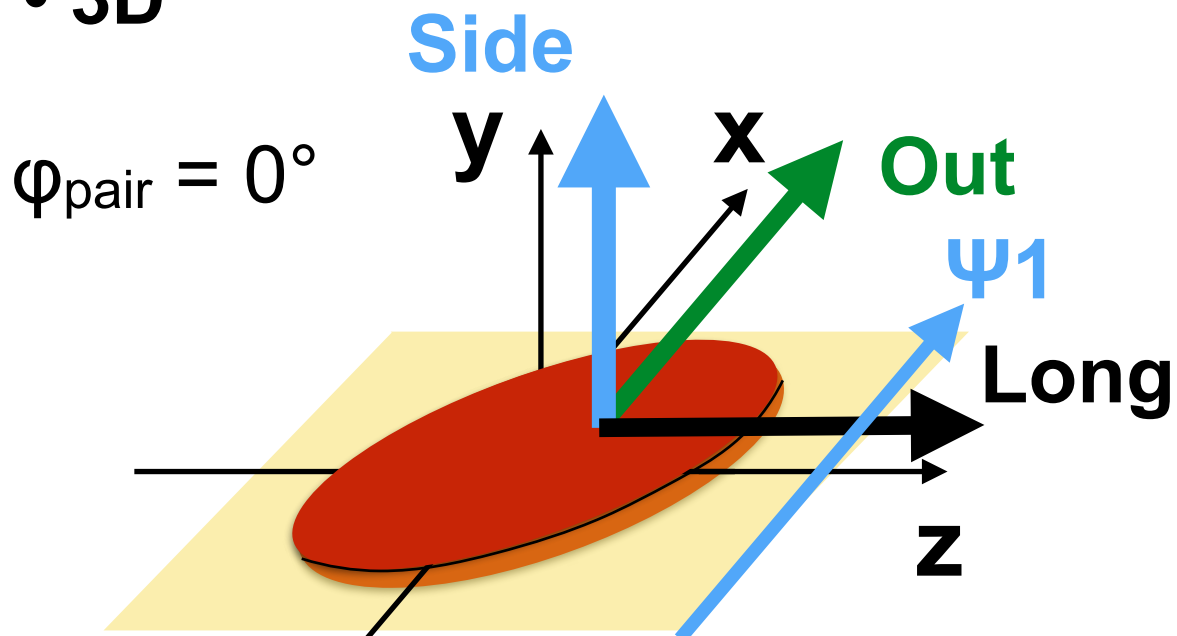
$$R_{ol}^2 \propto \cos(\phi)$$

$$R_{sl}^2 \propto \sin(\phi)$$

- R_{sl}^2 has its $+\pi/2$ oscillation

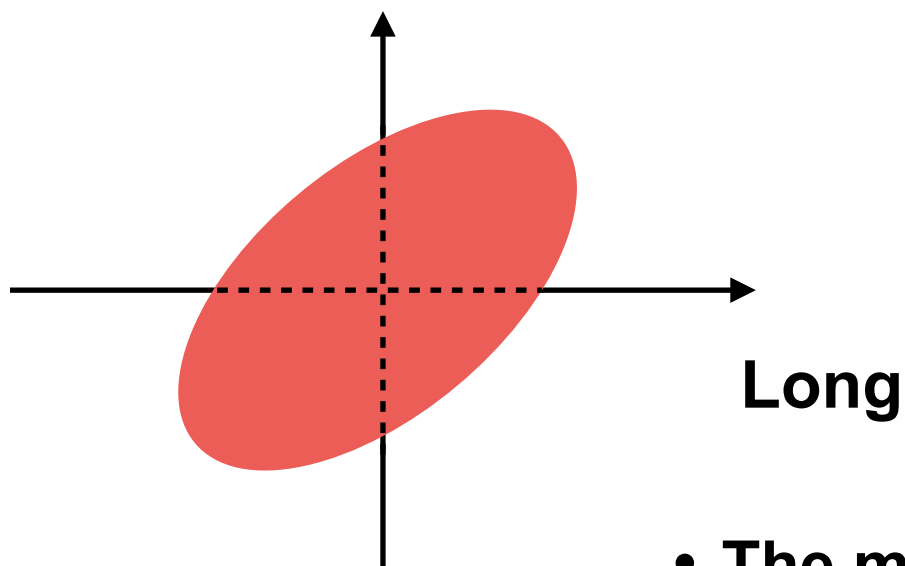
- The magnitude of oscillation corresponds to the tilt angle

• 3D



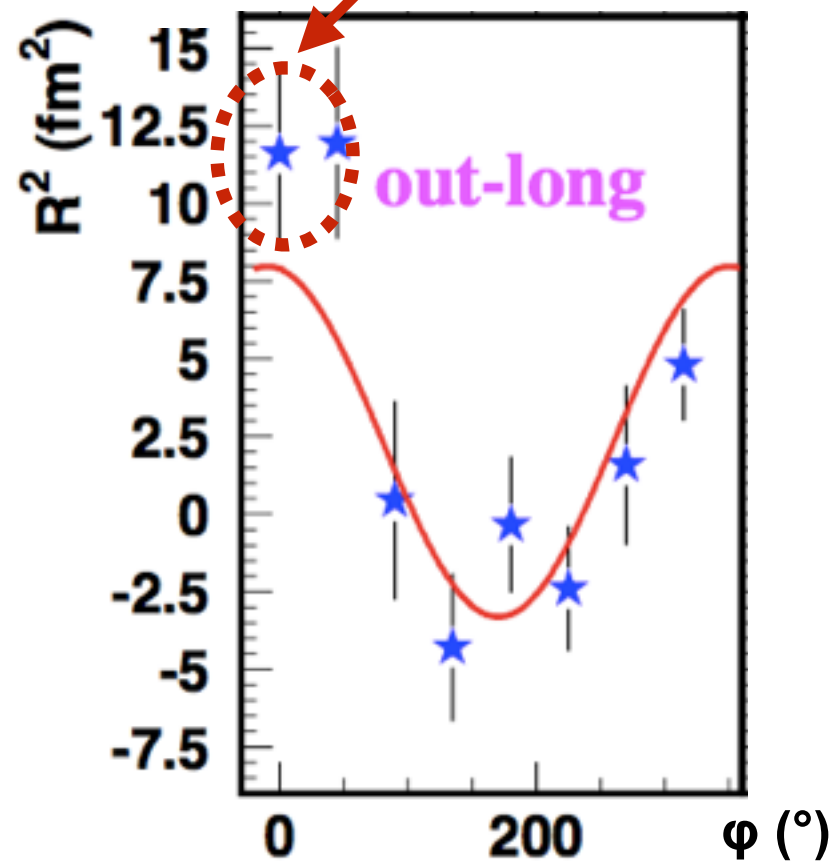
:Out - Long plane

• Projection Out - Long plane
Out



• The magnitude of oscillation corresponds to the tilt angle

$$R_{ol}^2 > 0$$

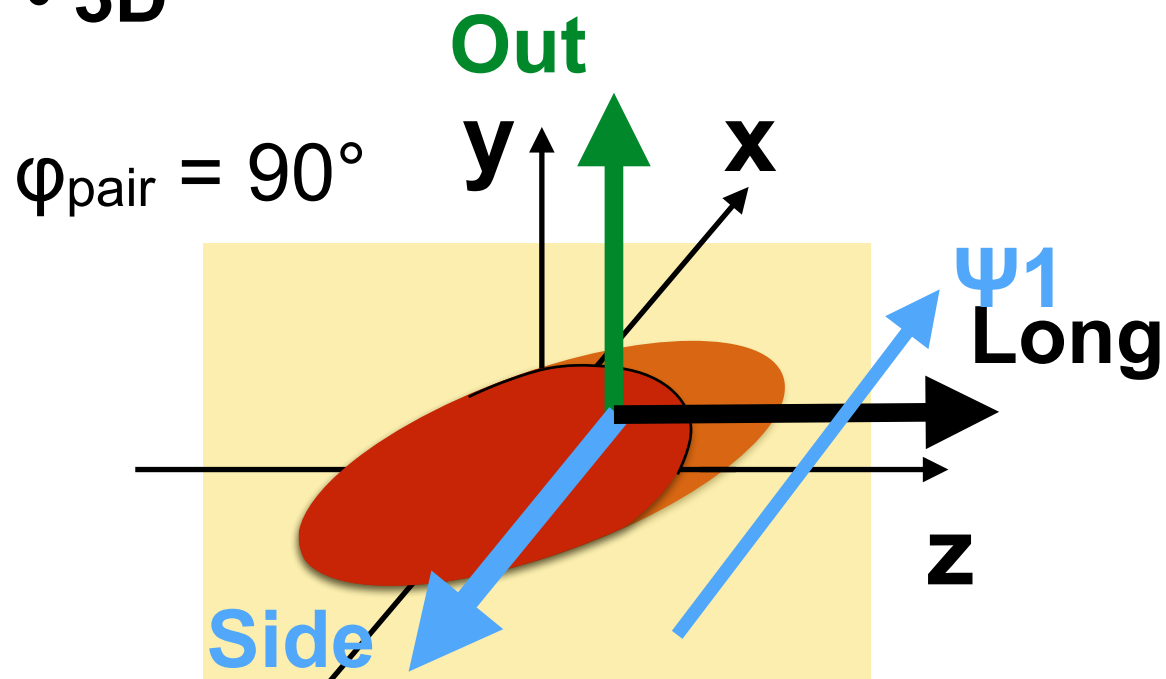


$$R_{ol}^2 \propto \cos(\phi)$$

$$R_{sl}^2 \propto \sin(\phi)$$

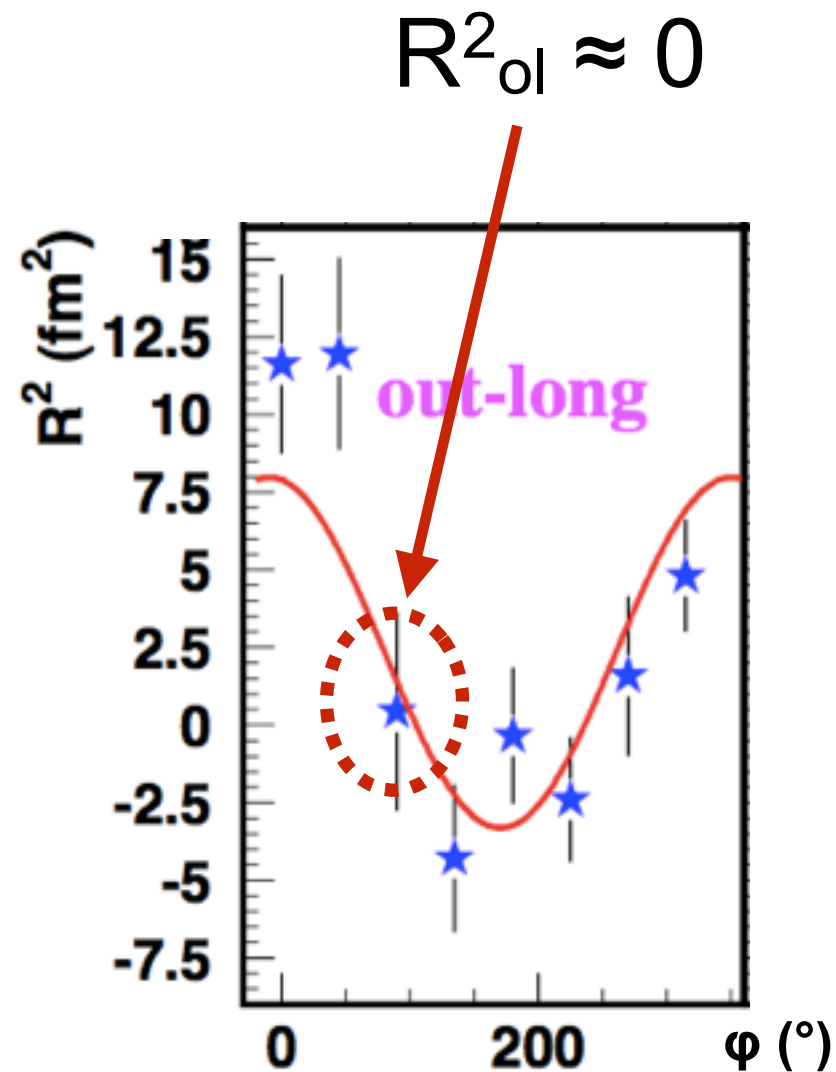
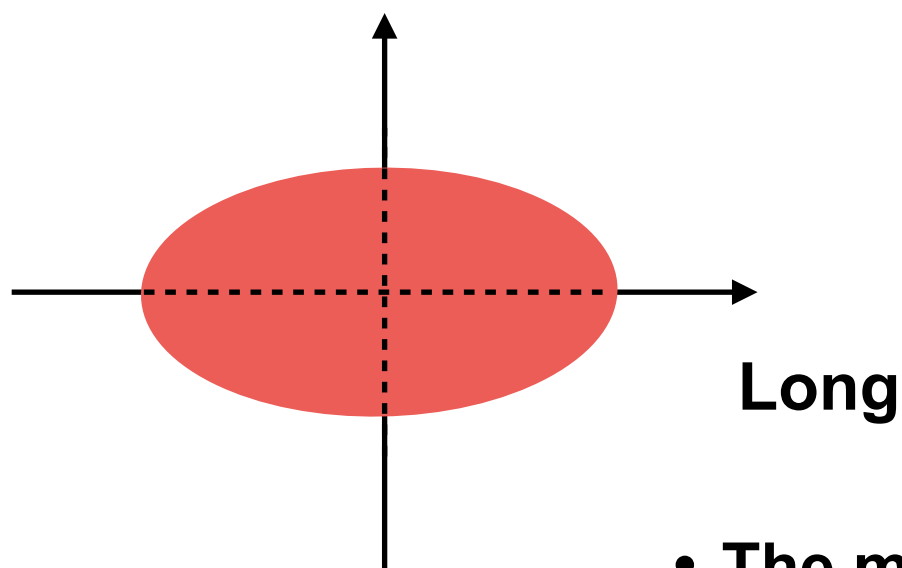
• R_{sl}^2 has its $+\pi/2$ oscillation

- 3D



:Out - Long plane

- Projection Out - Long plane



$$R_{ol}^2 \propto \cos(\phi)$$

$$R_{sl}^2 \propto \sin(\phi)$$

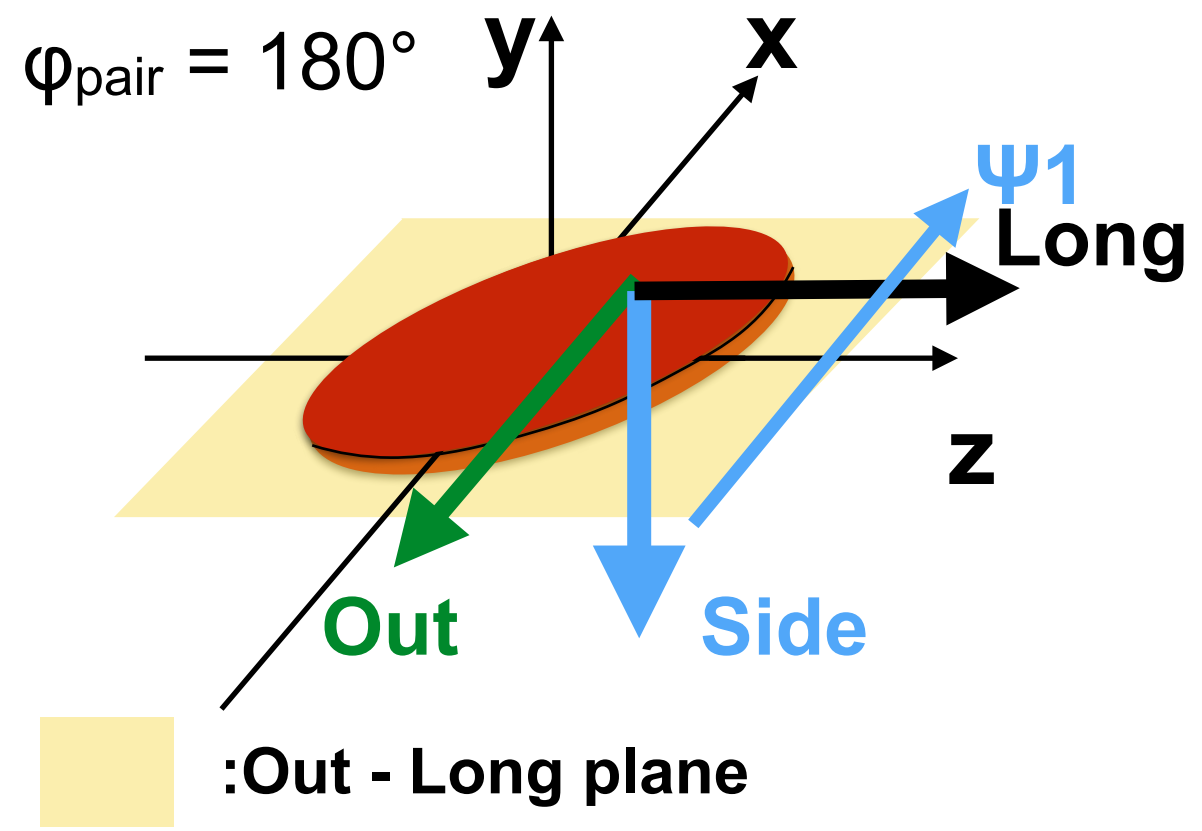
- R_{sl}^2 has its $+\pi/2$ oscillation

- The magnitude of oscillation corresponds to the tilt angle

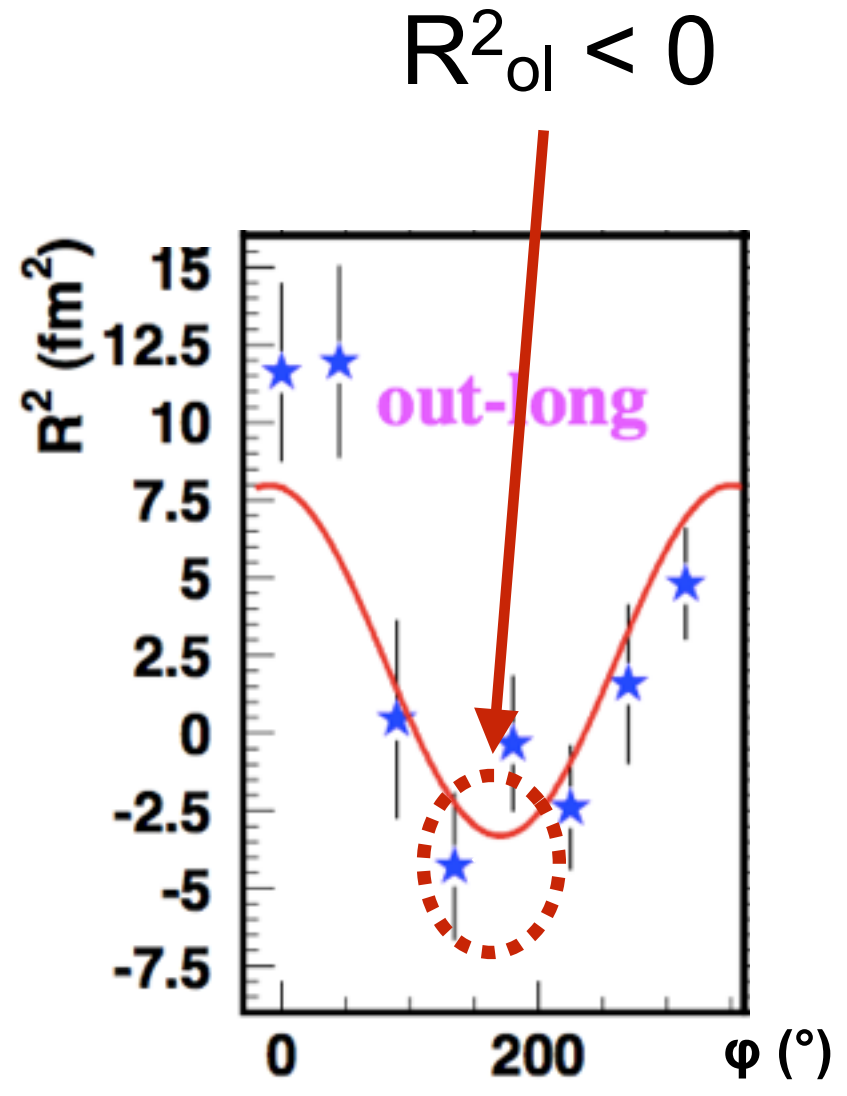
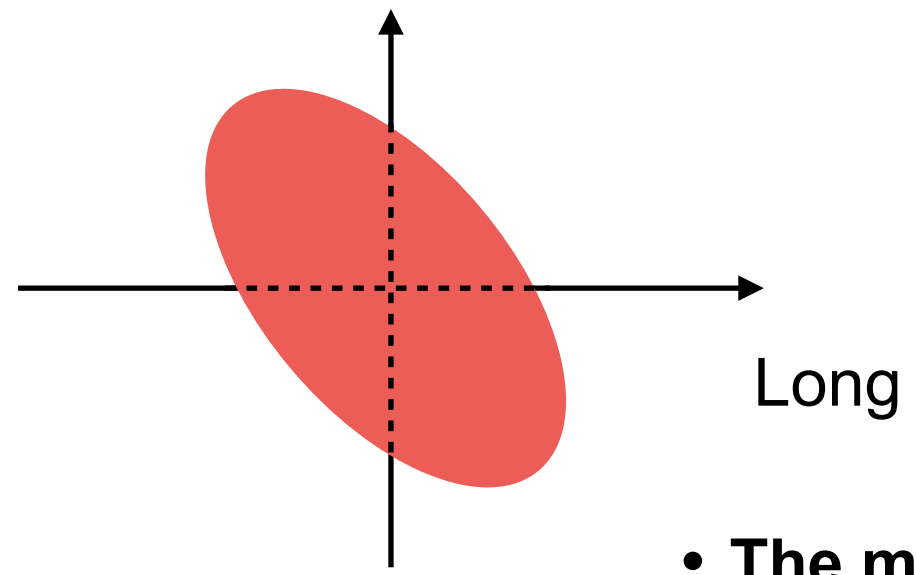


HBT radii w.r.t. Ψ_1

- 3D



- Projection Out - Long plane



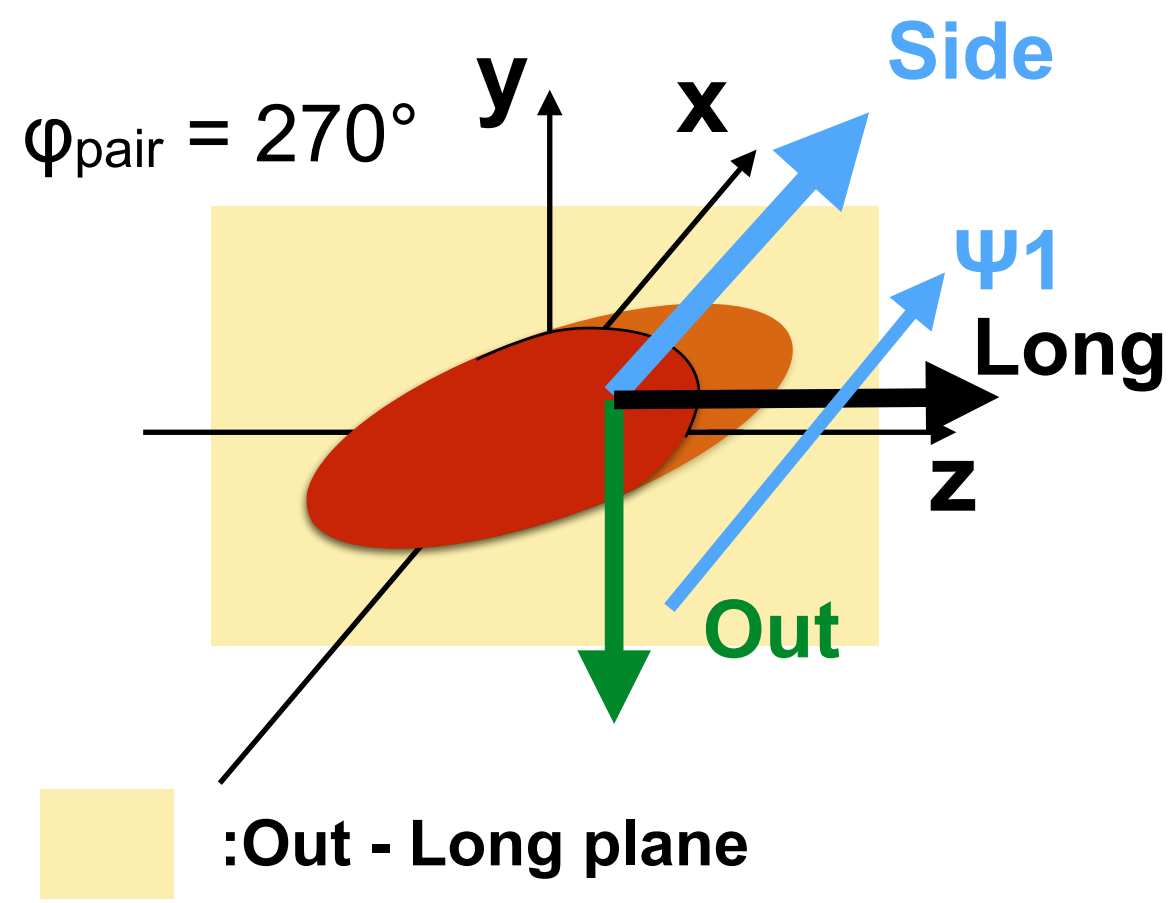
$$R_{ol}^2 \propto \cos(\phi)$$

$$R_{sl}^2 \propto \sin(\phi)$$

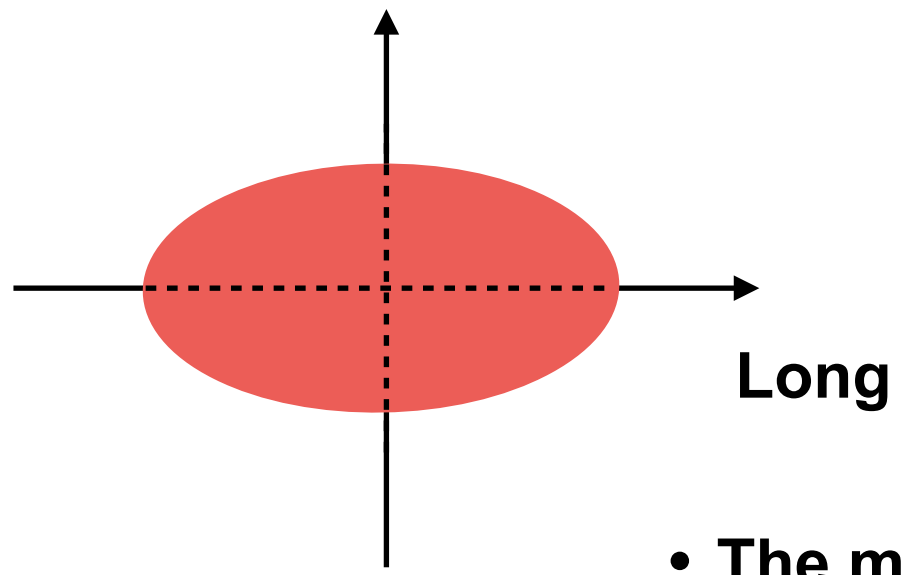
- R_{sl}^2 has its $+\pi/2$ oscillation

- The magnitude of oscillation corresponds to the tilt angle

- 3D

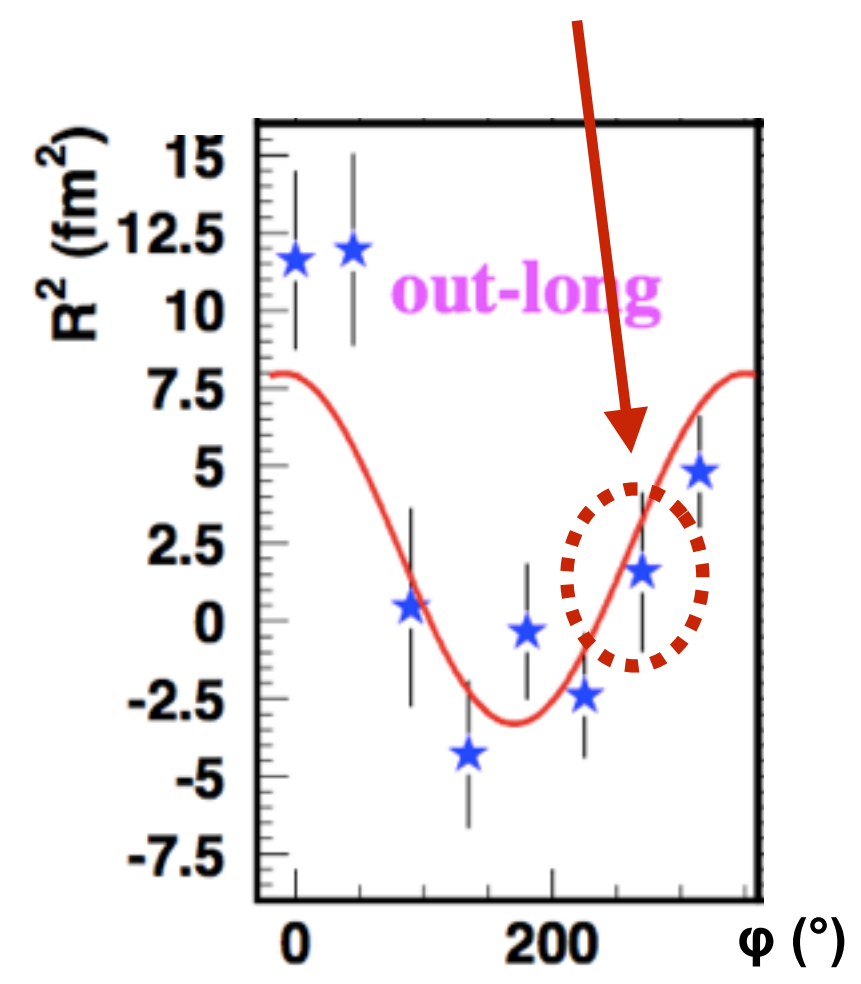


- Projection Out - Long plane



- The magnitude of oscillation corresponds to the tilt angle

$$R_{ol}^2 \approx 0$$



$$R_{ol}^2 \propto \cos(\phi)$$

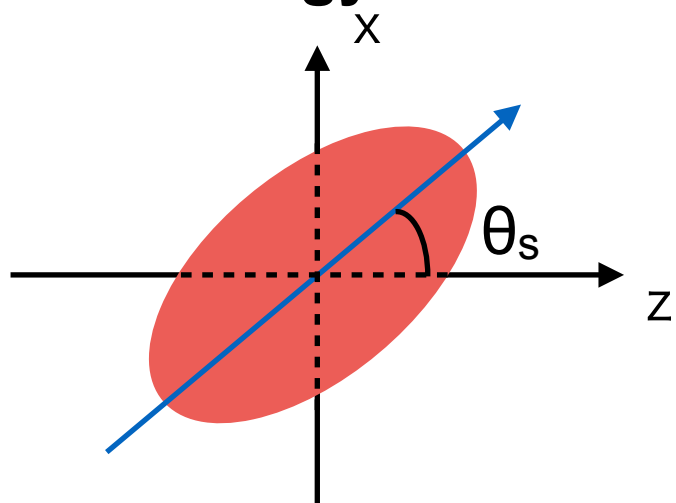
$$R_{sl}^2 \propto \sin(\phi)$$

- R_{sl}^2 has its $+\pi/2$ oscillation

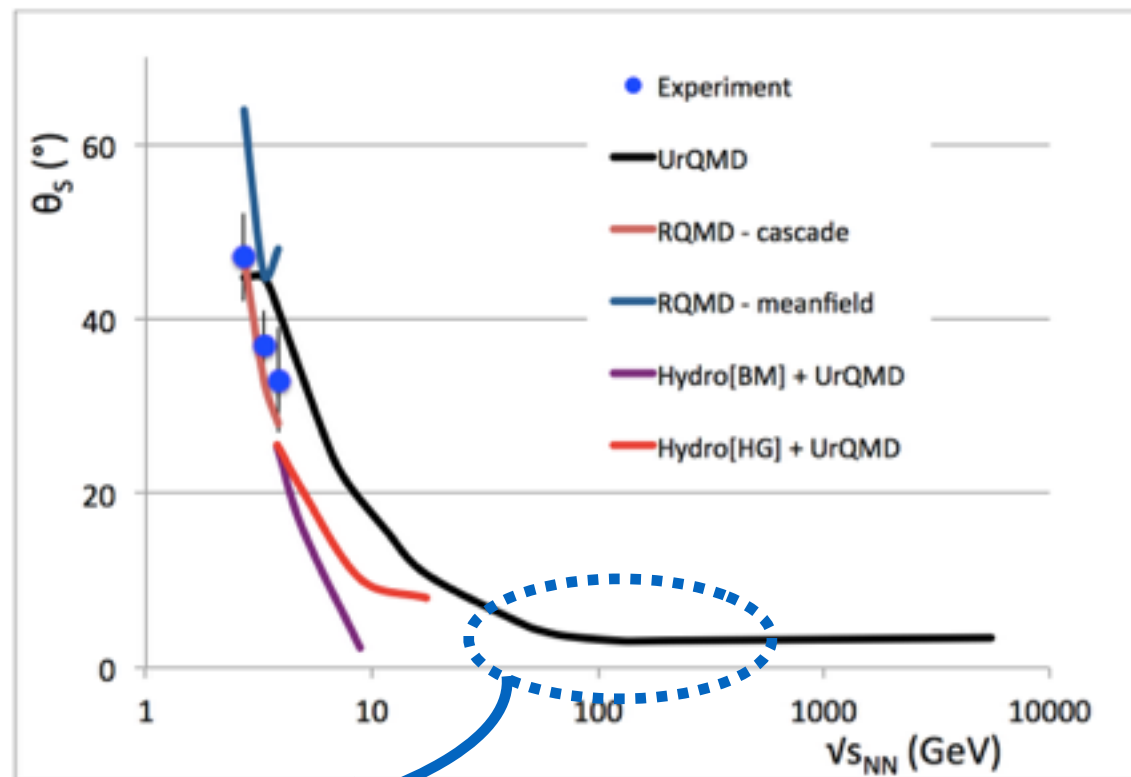
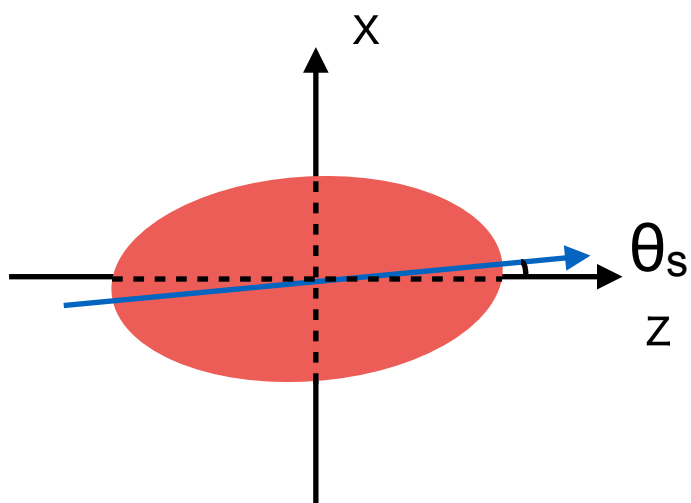


Motivation

✓ Low energy



✓ High energy expectation



Is there a signal ?

M. A. Lisa et al. New J. Phys. 13 (2011) 065006

Tilt angle

$$\theta_s = \frac{1}{2} \tan^{-1} \left(\frac{-4R_{sl,1}^2}{R_{l,0}^2 - R_{s,0}^2 + 2R_{s,2}^2} \right)$$

• Fit function:

$$R_{\mu,0}^2 + 2 R_{\mu,1}^2 \cos(\varphi - \Psi_1) + 2 R_{\mu,2}^2 \cos(2(\varphi - \Psi_1)) , (\mu = o, s, ol)$$

$$R_{\mu,0}^2 + 2 R_{\mu,1}^2 \sin(\varphi - \Psi_1) + 2 R_{\mu,2}^2 \sin(2(\varphi - \Psi_1)) , (\mu = os, sl)$$

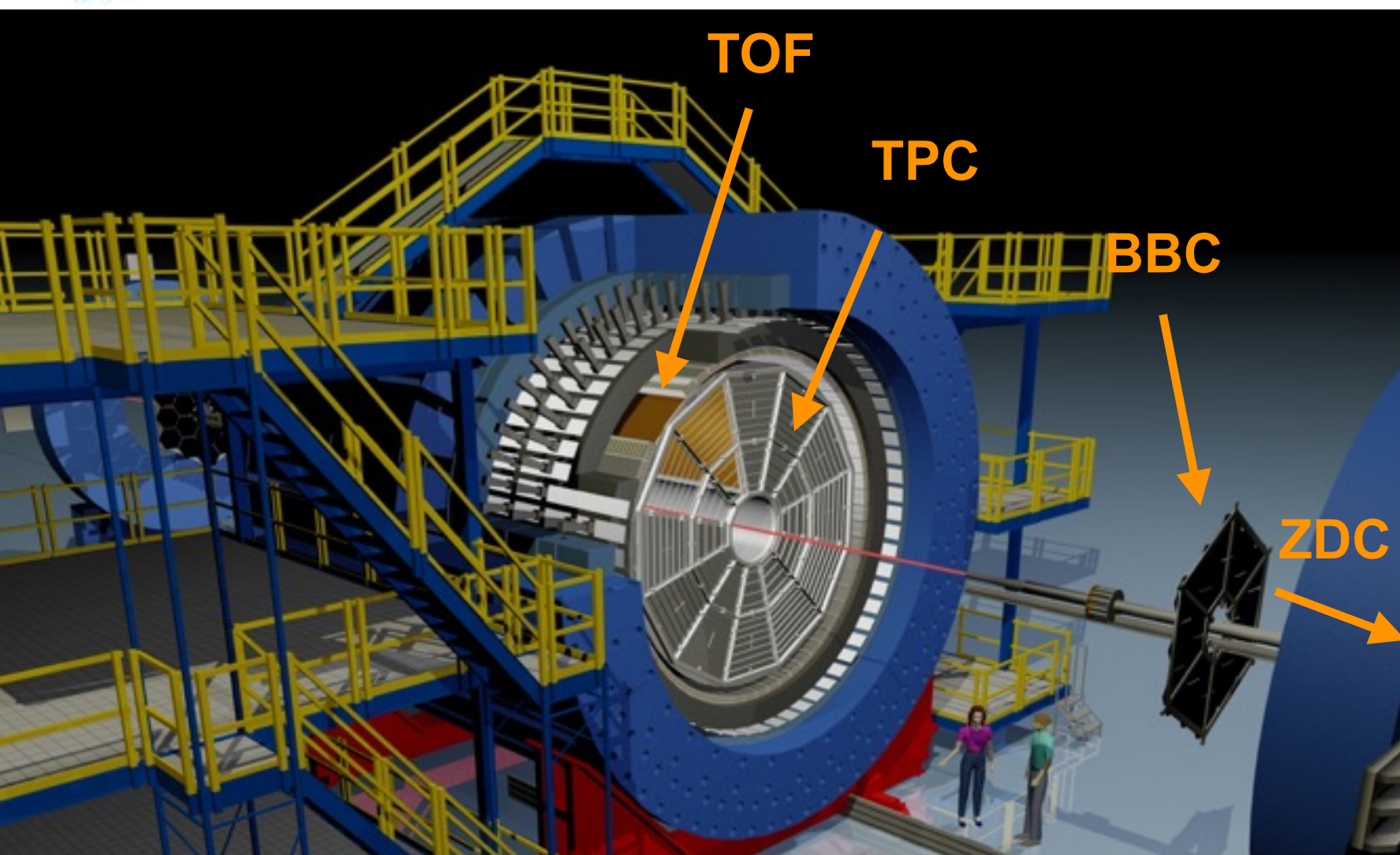
- Experimentally, source tilt has been only measured at low energies
- Tilt angle is inversely proportional to the beam energy
- At RHIC energy (200 GeV), source tilt value is expected to be nearly 0 or signal is very small

✓ Perform HBT measurement w.r.t Ψ_1 and scope tilt signal

using both Au+Au and Cu+Au in 200 GeV

✓ Cu+Au have initial density asymmetry...

-> How does it affect HBT measurement?



Time Projection Chamber (TPC)

- Main tracking detector, $|\eta| < 1.0$, full azimuth

Zero Degree Calorimeter (ZDC)

- $|\eta| > 6.3$
- Measure spectator neutron
- Event plane reconstruction using spectator neutrons

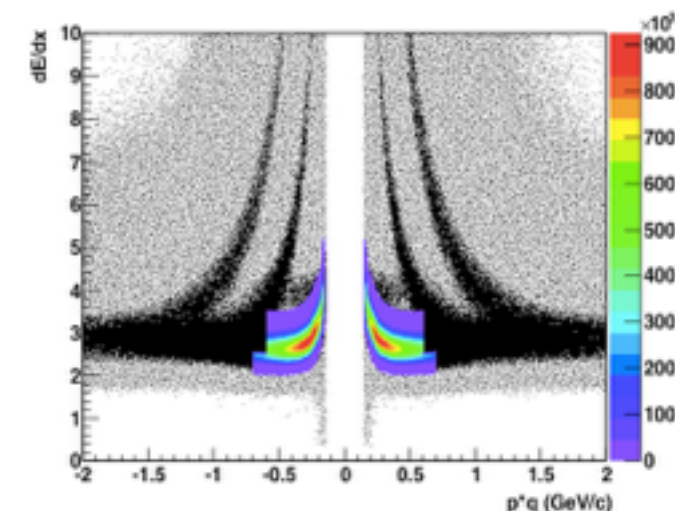
Beam-Beam Counters (BBC)

- $3.3 < |\eta| < 5$
- Event plane reconstruction using participants

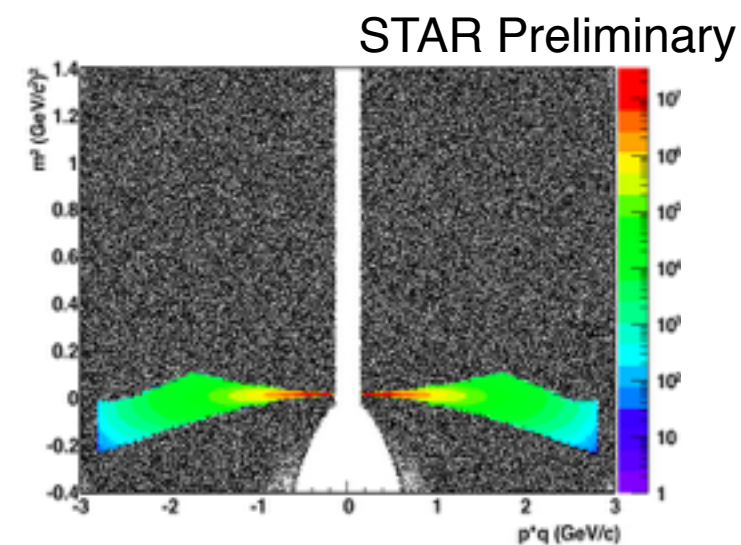
TOF & TPC detector

✓ Use PID (particle identification)

TPC (dE/dx) STAR Preliminary



TOF (time of flight) STAR Preliminary



✓ Pion selected

STAR Analysis

- Au+Au 200 GeV, Cu+Au 200 GeV
- Number of events: Au+Au ~ 430 M
Cu+Au ~ 45 M
- Correlation function

$$C(q) = \frac{N(q)}{D(q)}$$

N: pair distribution from the same event (real)
D: different event pair distribution from the different events (mixed)

- Estimate Coulomb interaction correction factor
K(q) : Coulomb correction factor
- Fit correlation function and extract radii parameters

$$C(\vec{q}) = N[(1 - \lambda) + \lambda K(q)(1 + G(\vec{q}))]$$

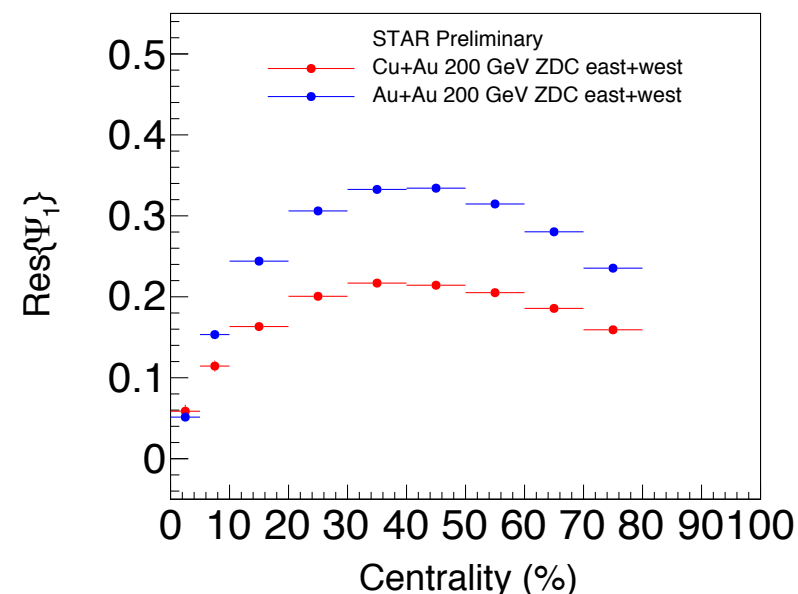
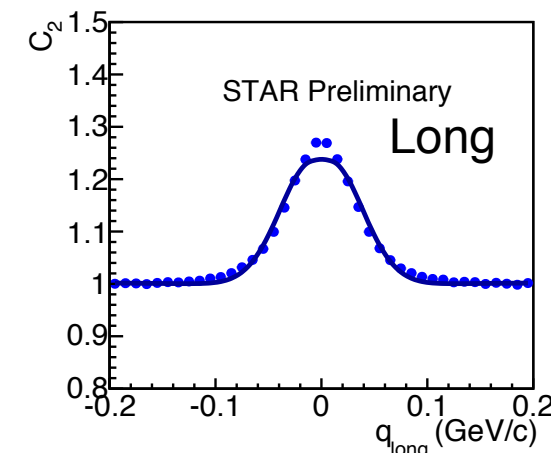
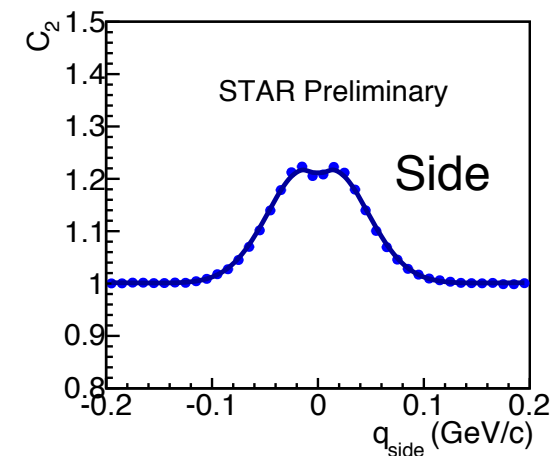
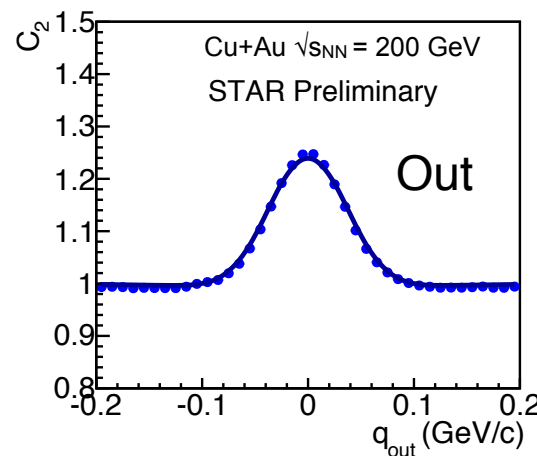
✓ Azimuthally-integrated analysis

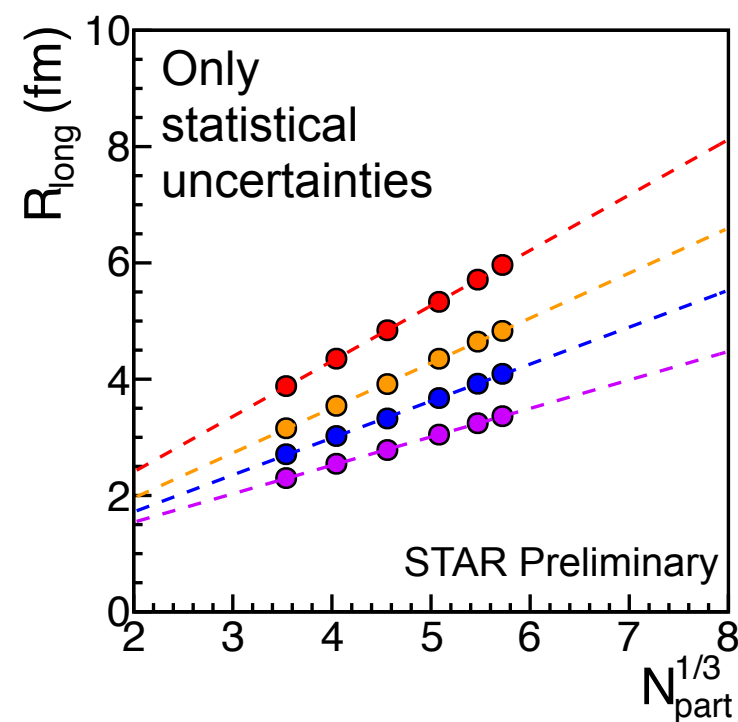
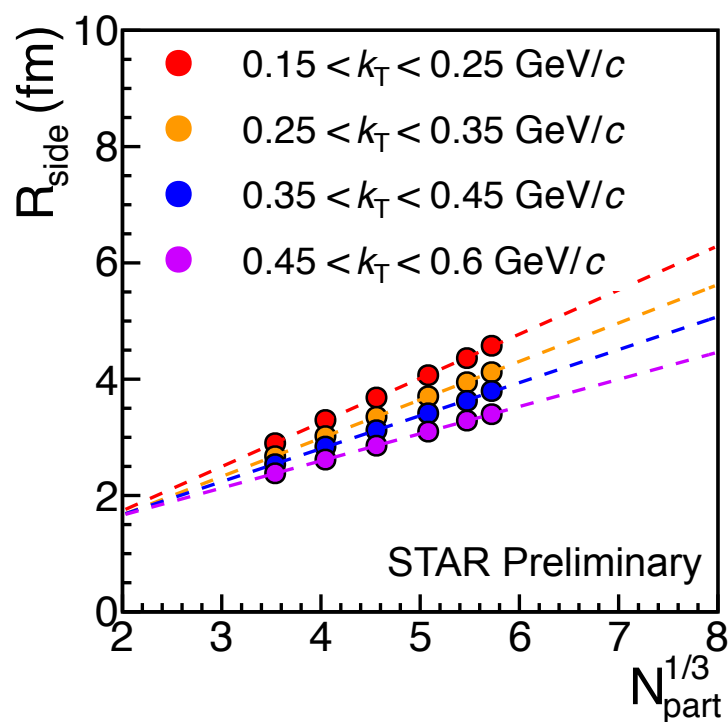
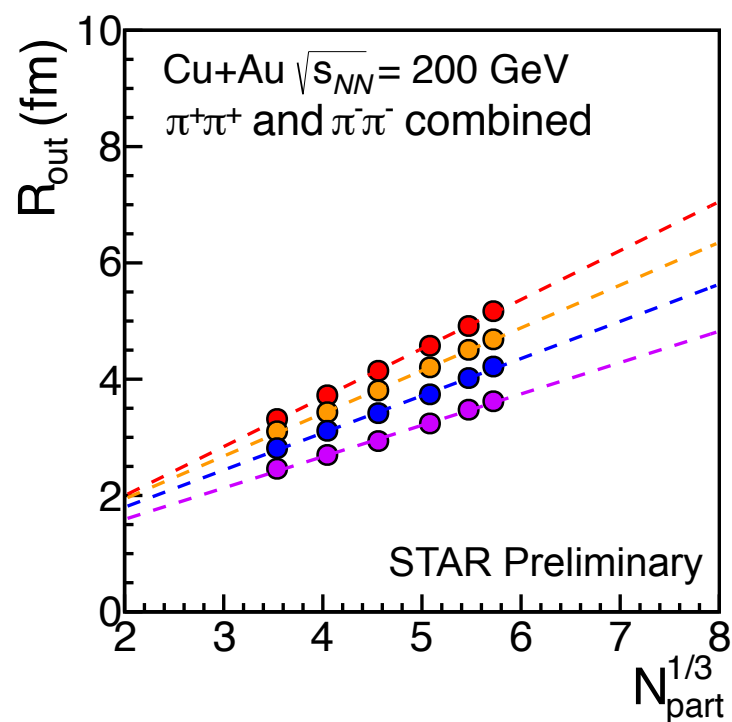
$$G(\vec{q}) = \exp(-R_{out}^2 q_{out}^2 - R_{side}^2 q_{side}^2 - R_{long}^2 q_{long}^2)$$

✓ Azimuthal-angle-dependent HBT analysis

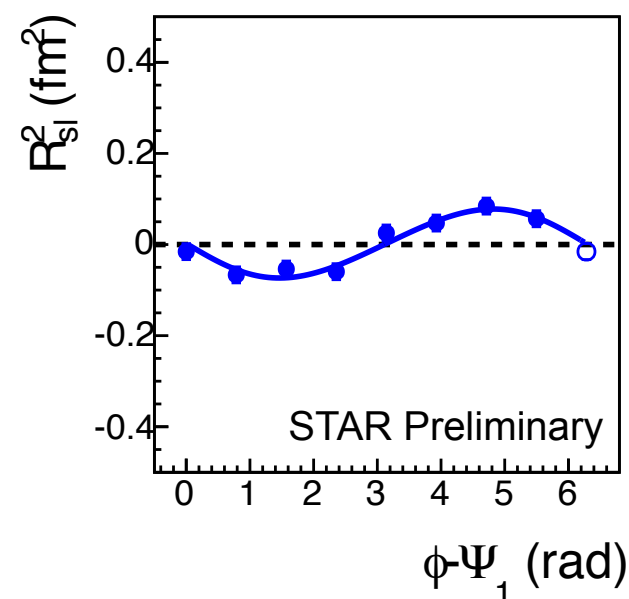
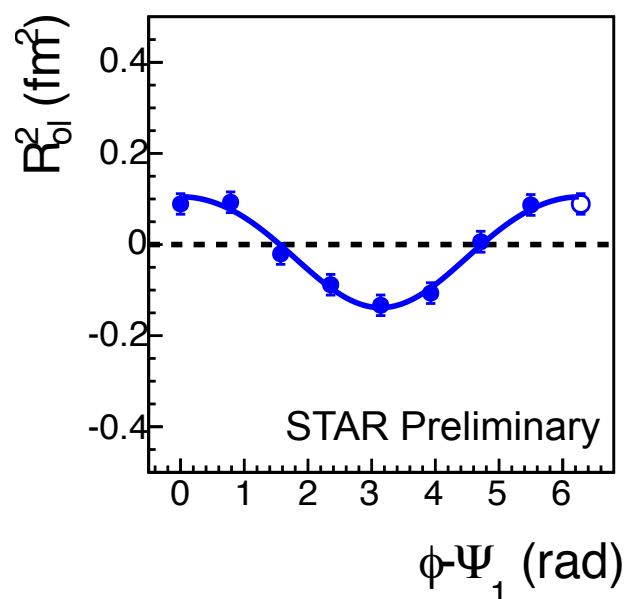
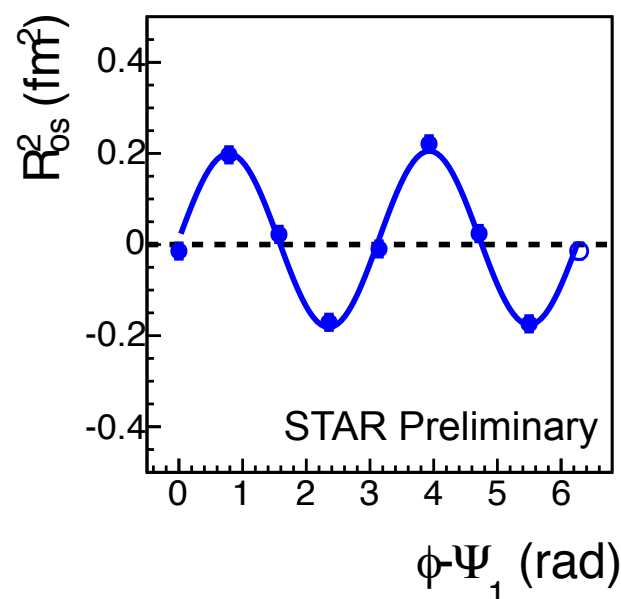
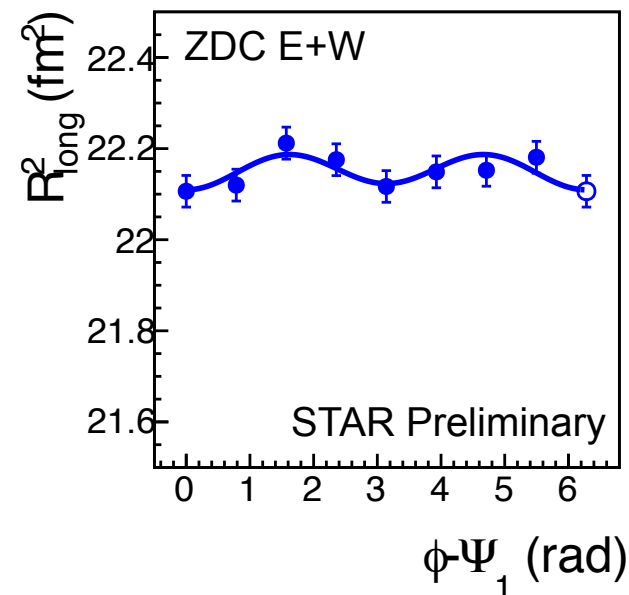
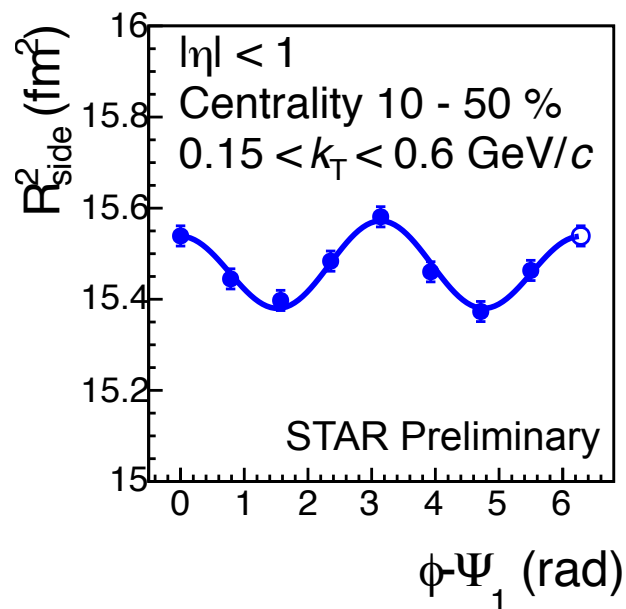
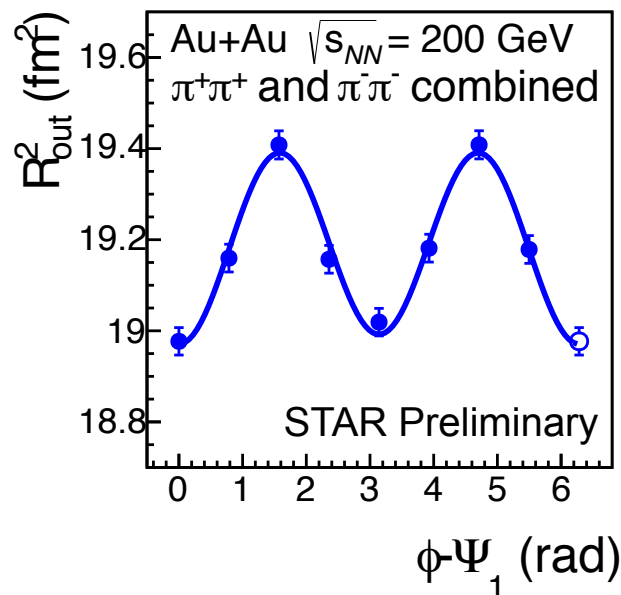
$$G(\vec{q}) = \exp(-R_{out}^2 q_{out}^2 - R_{side}^2 q_{side}^2 - R_{long}^2 q_{long}^2 - 2R_{os}^2 q_{out} q_{side} - 2R_{ol}^2 q_{out} q_{long} - 2R_{sl}^2 q_{side} q_{long})$$

- Event plane reconstruction
✓ ZDC east + west plane used
Res Ψ_1 ~ 0.35 (Au+Au)
Res Ψ_1 ~ 0.20 (Cu+Au)





- $N_{part}^{1/3}$ corresponds to the source radius at the collision time
- Checked HBT radii $\propto N_{part}^{1/3}$



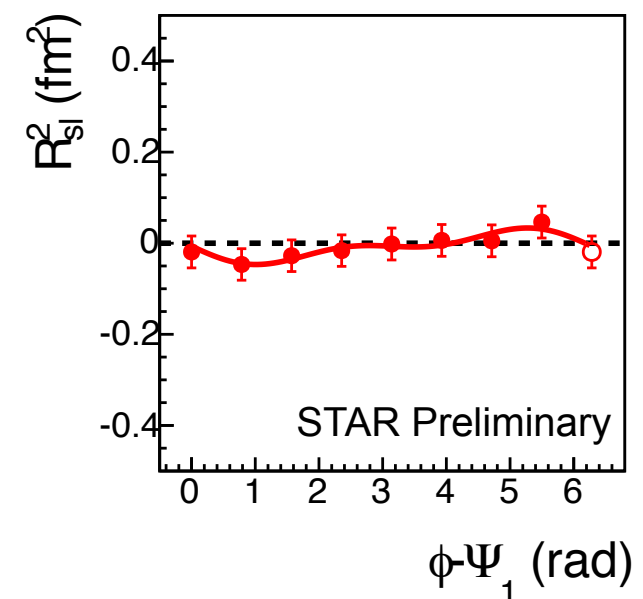
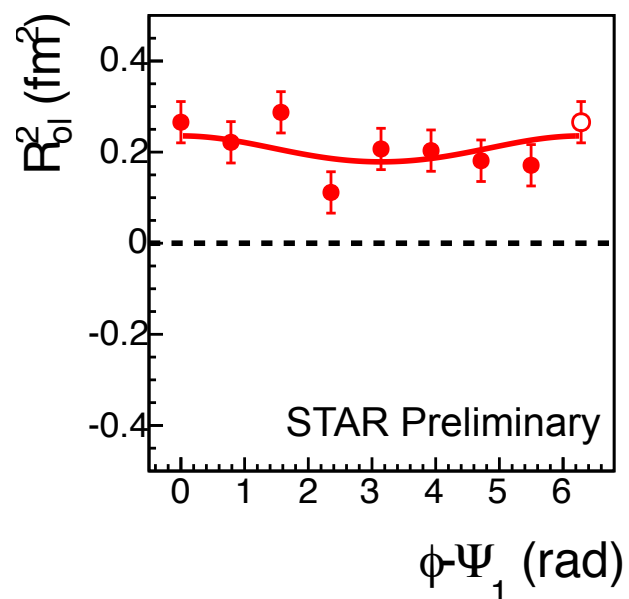
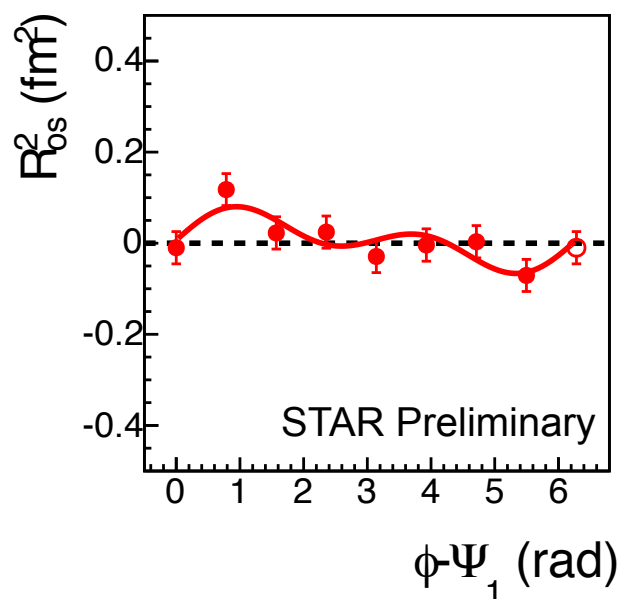
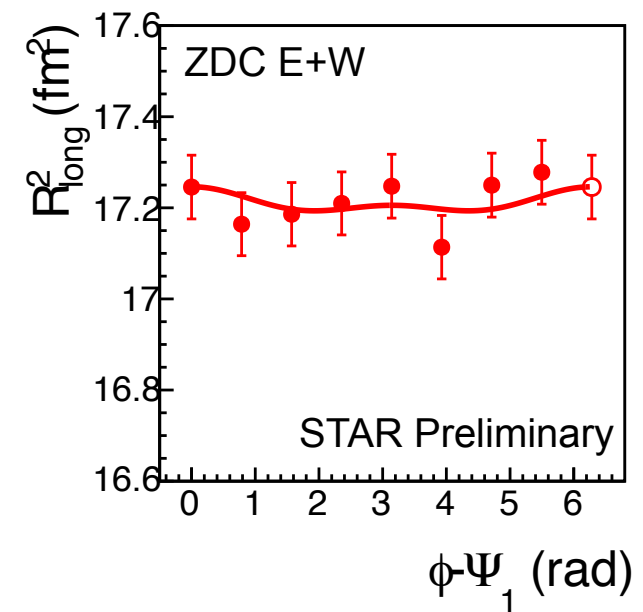
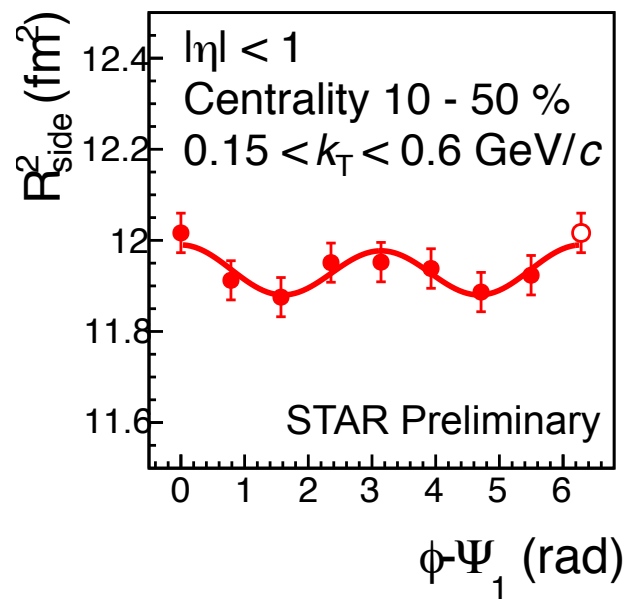
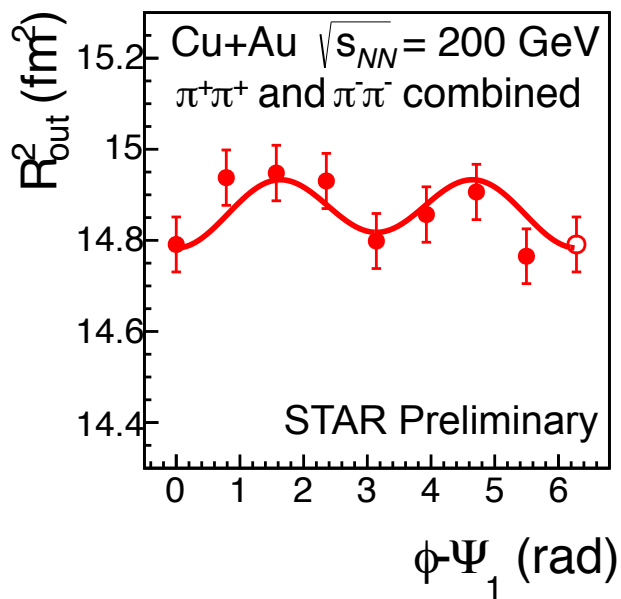
• EP resolution correction is not applied

- R_{out} , R_{side} and R_{os} have a 2nd-order oscillation due to the elliptic source shape with respect to Ψ_1
- Small (but $\neq 0$) 1st-order oscillation can be found in R_{ol} and R_{sl} due to the source tilt signal
- These results indicate that the source shape at freeze-out is tilted even at the top RHIC energy

• Note that $\phi - \Psi_1 = 0$ point is replotted at $\phi - \Psi_1 = 2\pi$



HBT radii w.r.t. Ψ_1 in Cu+Au



• EP resolution correction is not applied

- In R_{oi} , average magnitude is shifted from 0 because center-of-mass rapidity is not 0 (shift to Au-going side ($\eta < 0$))
 - Oscillation sign is similar trend with Au+Au
 - Oscillation is distorted -> simply due to the poor EP resolution? or density asymmetry affects and distorts oscillation ?
- > More statistics may reveal where this trend comes from



Event plane resolution correction

- Fit function:

$$R^2_{\mu,0} + 2 R^2_{\mu,1} \cos(\varphi - \Psi_1) + 2 R^2_{\mu,2} \cos(2(\varphi - \Psi_1)) , (\mu = o, s, ol)$$

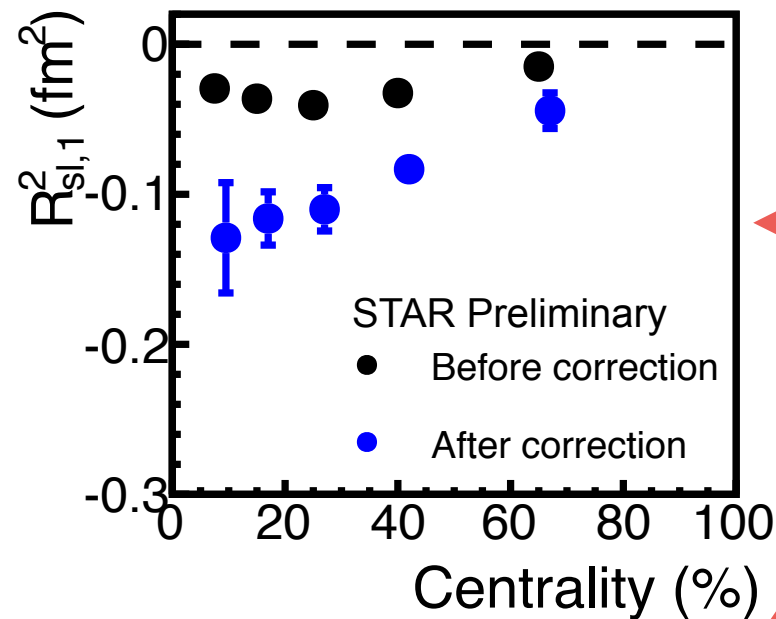
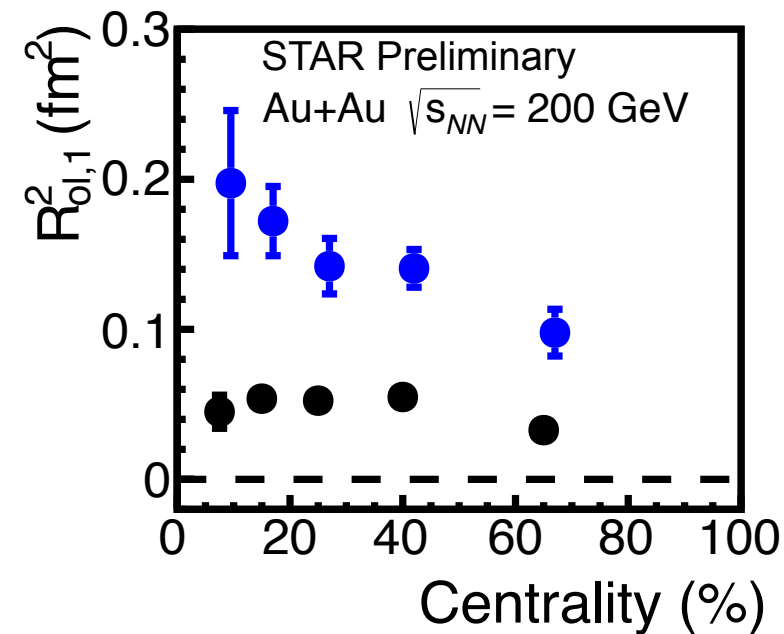
$$R^2_{\mu,0} + 2 R^2_{\mu,1} \sin(\varphi - \Psi_1) + 2 R^2_{\mu,2} \sin(2(\varphi - \Psi_1)) , (\mu = os, sl)$$

$$R^2_{\mu,n}{}^{true} = R^2_{\mu,n}{}^{obs} \times \frac{n\Delta/2}{\sin(n\Delta/2) \langle \cos(n(\Psi_1 - \Psi_R)) \rangle}$$

Correction is applied by dividing EP resolution (for 1st- and 2nd-order resolution)

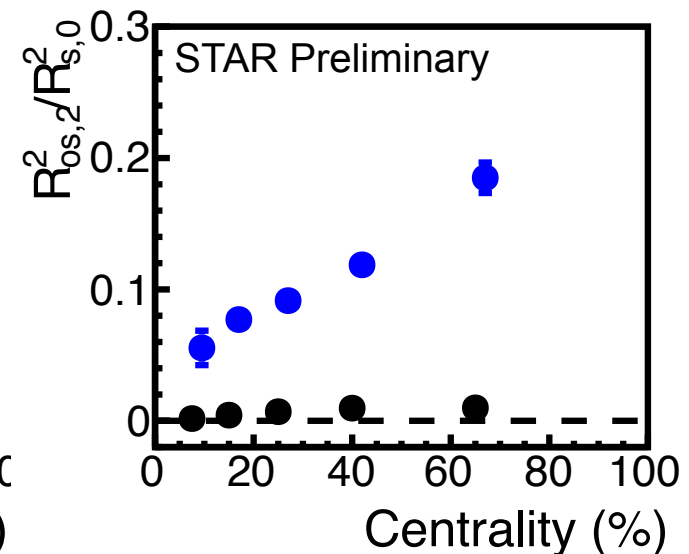
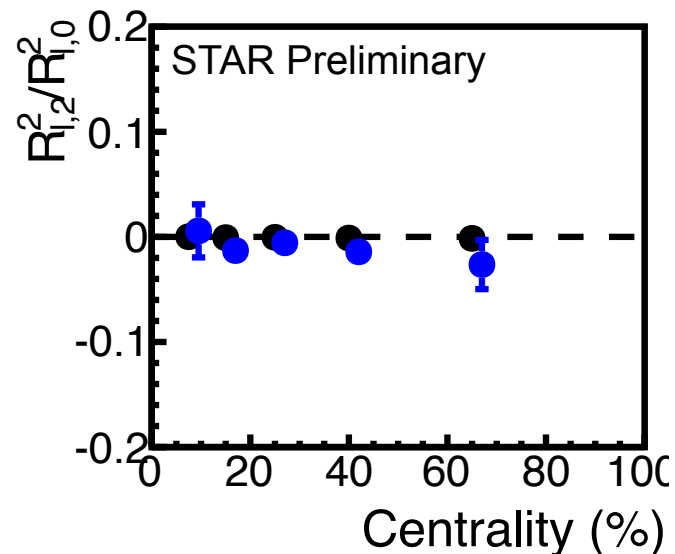
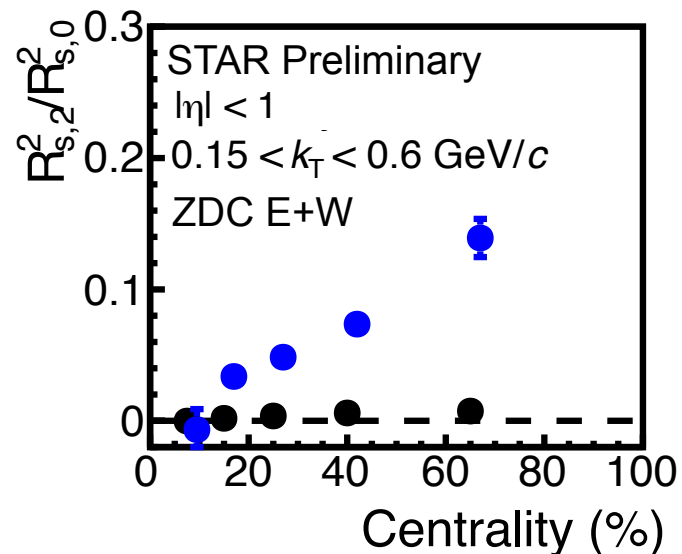
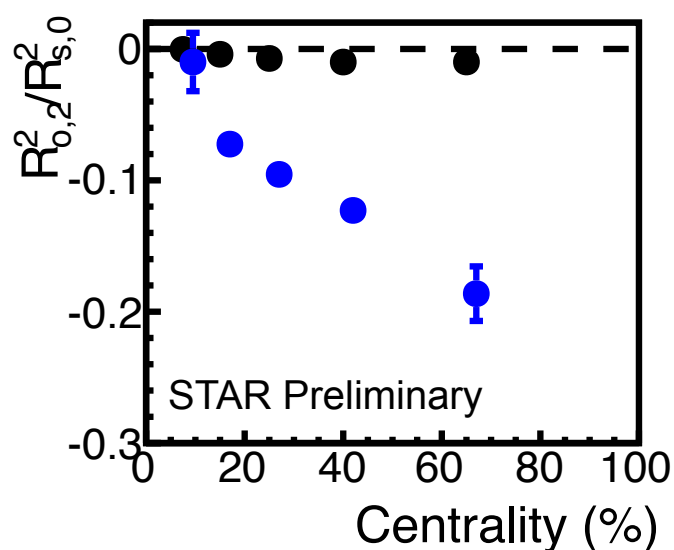
together with finite azimuthal angle bin width correction

- 1st-order oscillations



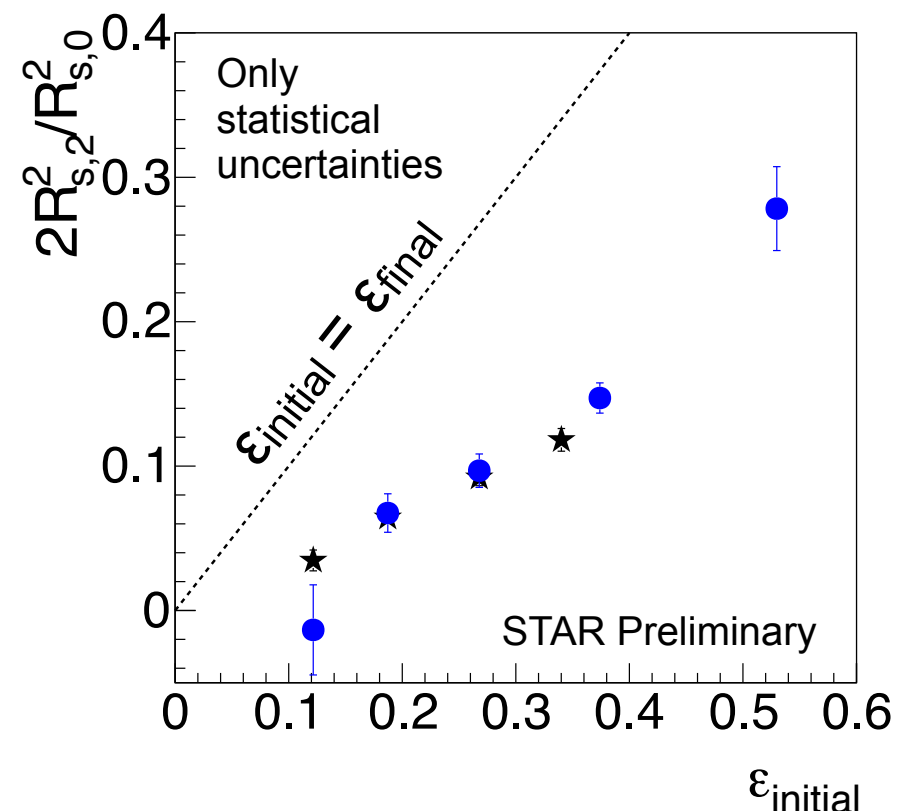
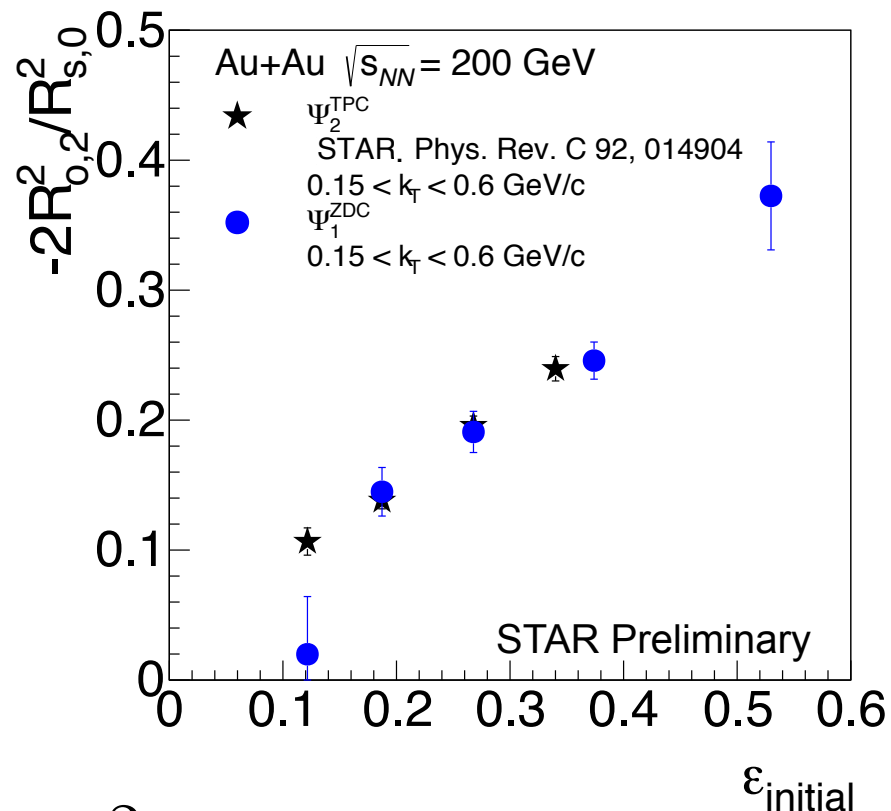
• The 1st-order oscillations decrease with increasing centrality
 • The 2nd-order oscillations increase with increasing centrality

- The 2nd-order oscillations relative to the average radii



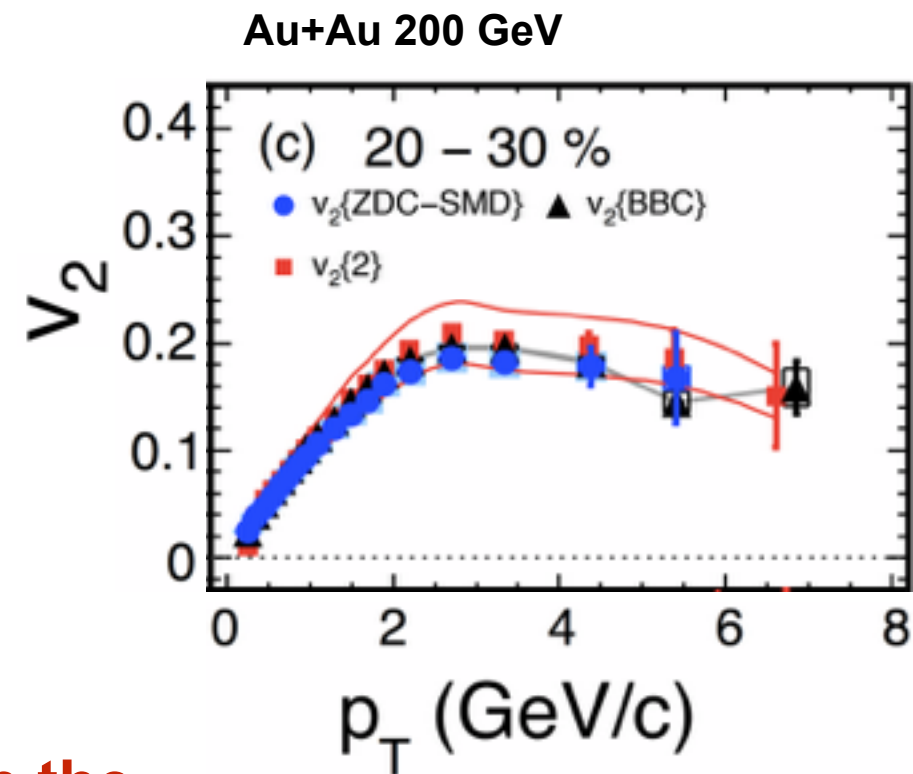


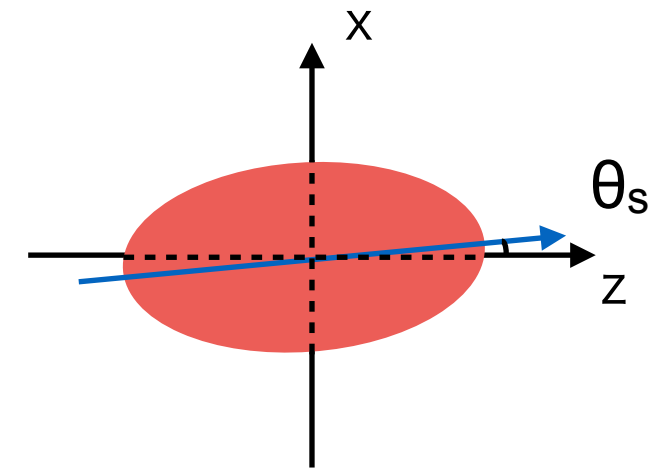
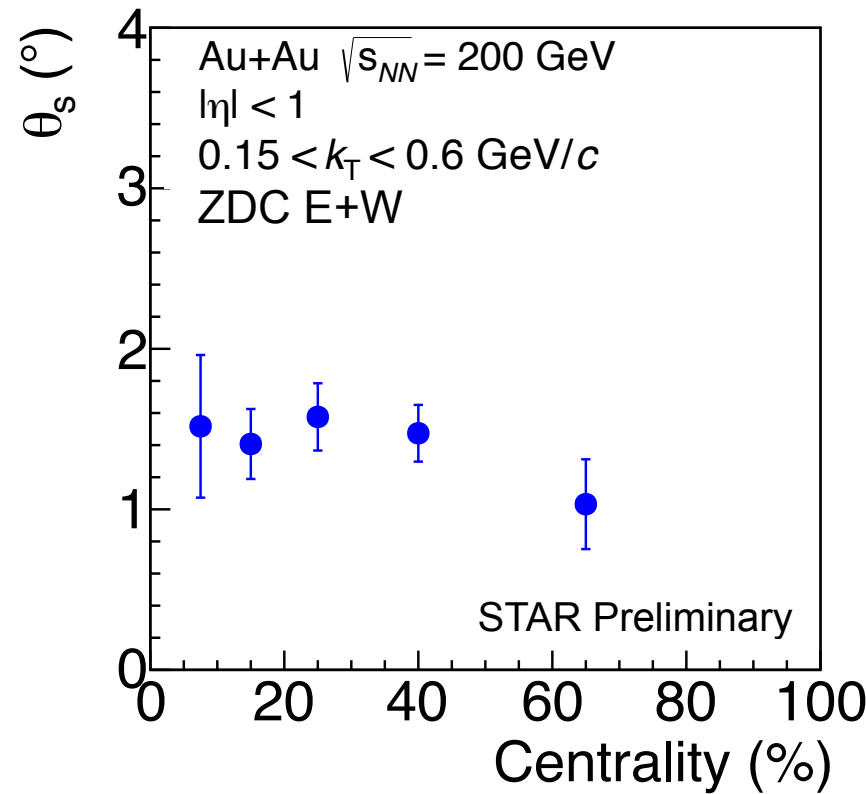
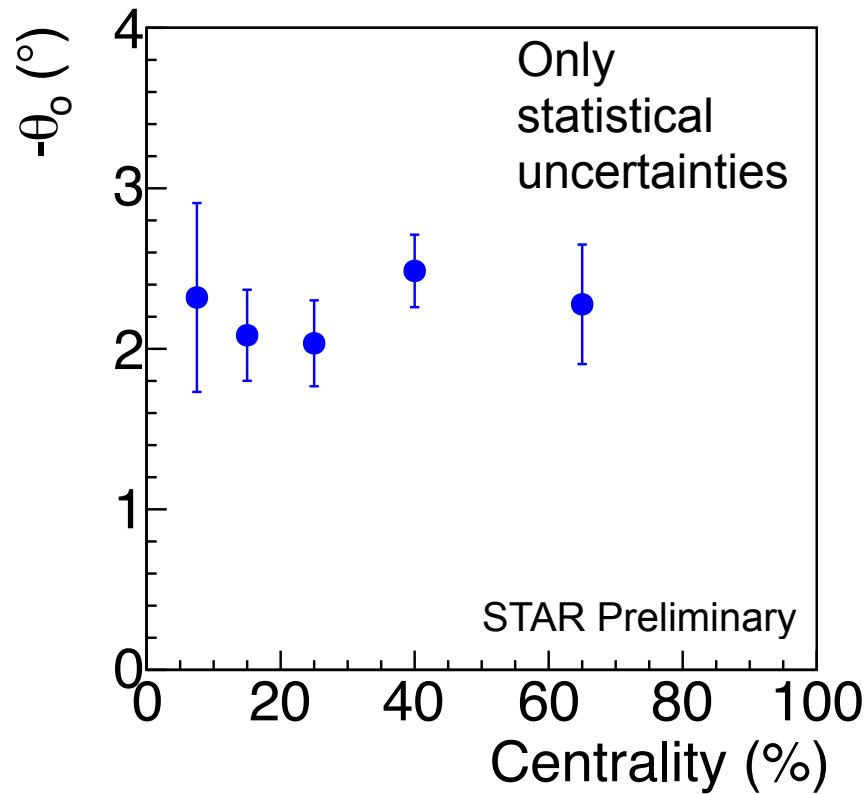
Final eccentricity w.r.t. $\Psi_1(\text{ZDC})$ vs $\Psi_2(\text{TPC})$



$$\epsilon_{\text{final}} \approx 2 \frac{R_{s,2}^2}{R_{s,0}^2} \quad \bullet \quad \epsilon_{\text{initial}} \text{ is from the Glauber simulation}$$

- Final eccentricity ϵ_{final} w.r.t. Ψ^{ZDC}_1 is measured
- $2R_{s,2}^2/R_{s,0}^2$ purely corresponds final eccentricity ϵ_{final}
- Momentum space anisotropy is same ($v_2\{2\} \approx v_2\{\text{ZDC}\}$) at low p_T
- Final eccentricity is smaller than initial eccentricity, but still remain out-of-plane extended ($\epsilon_{\text{final}} > 0$)
- Final eccentricity shows a rough agreement between the participant Ψ_2 and the spectator Ψ_1 planes



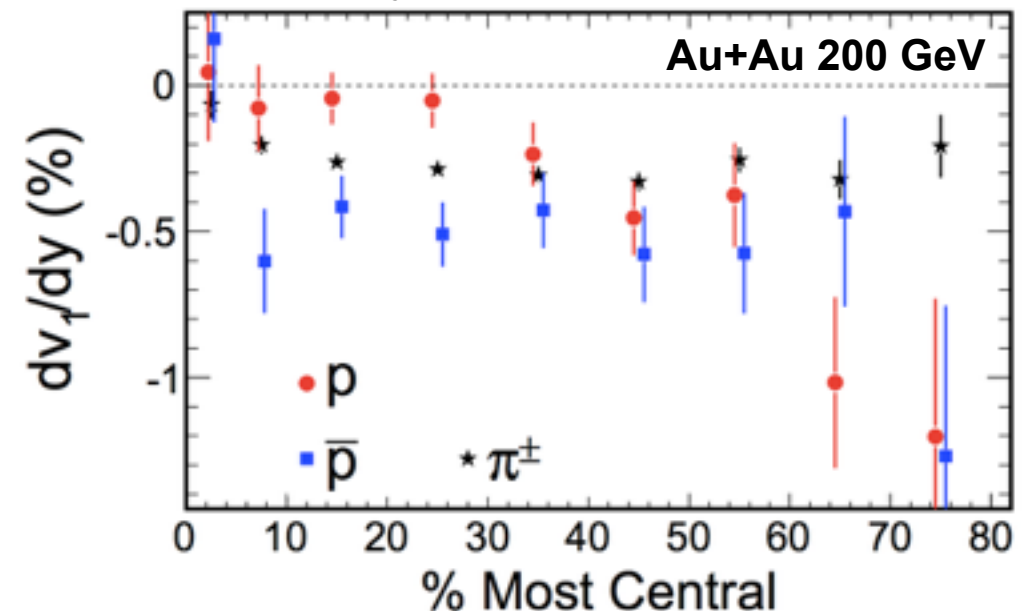


STAR Collaboration,
Phys. Rev. Lett. 108, (2012) 202301

Tilt angle

$$\theta_s = \frac{1}{2} \tan^{-1} \left(\frac{-4R_{sl,1}^2}{R_{l,0}^2 - R_{s,0}^2 + 2R_{s,2}^2} \right)$$

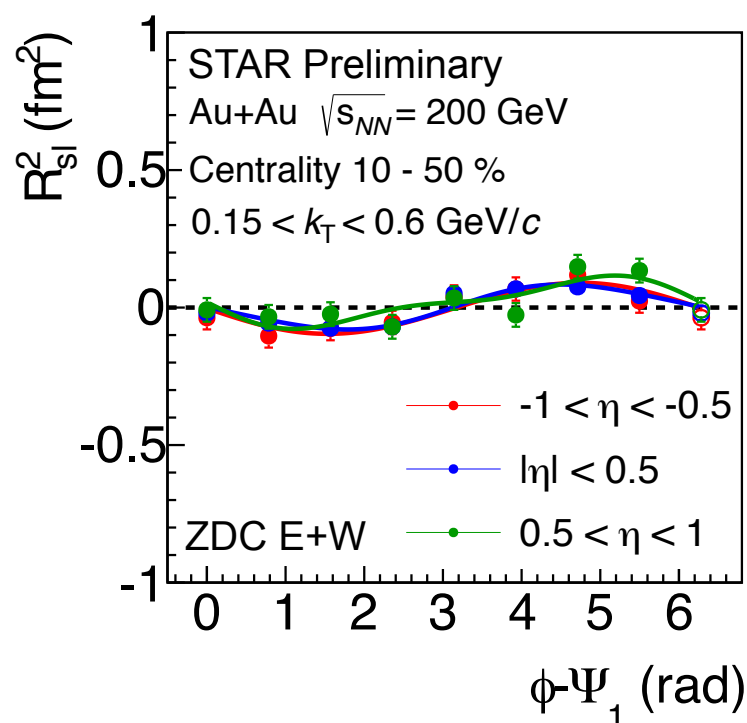
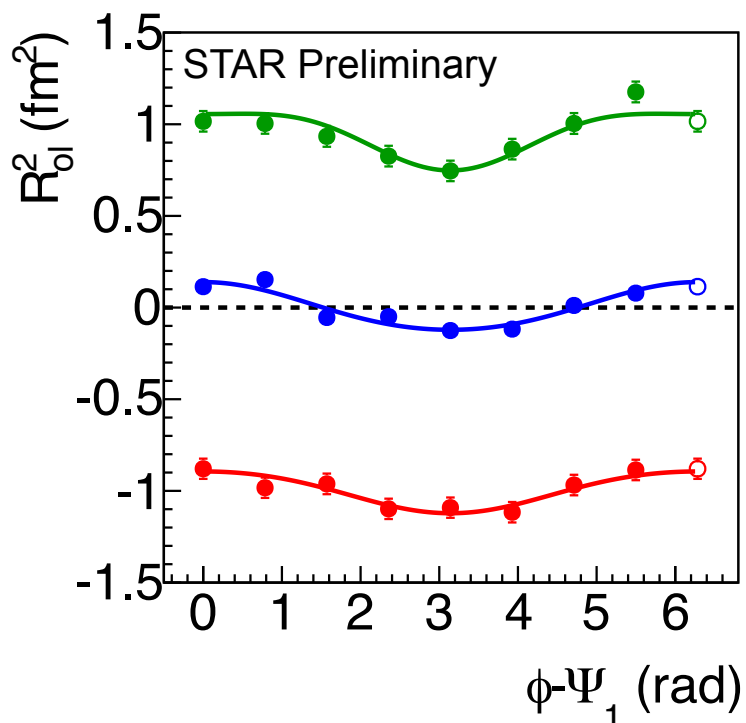
$$\theta_o = \frac{1}{2} \tan^{-1} \left(\frac{-4R_{ol,1}^2}{R_{l,0}^2 - R_{s,0}^2 + 2R_{s,2}^2} \right)$$



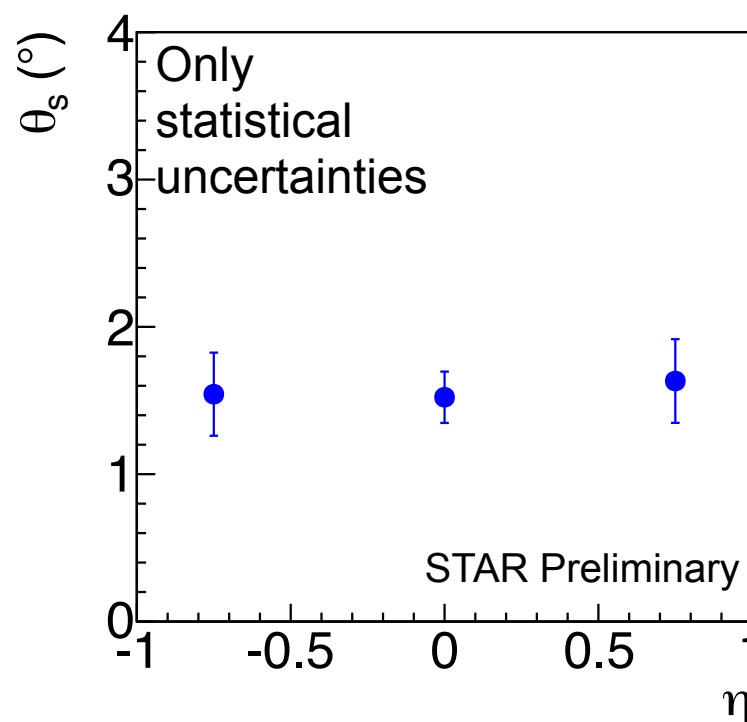
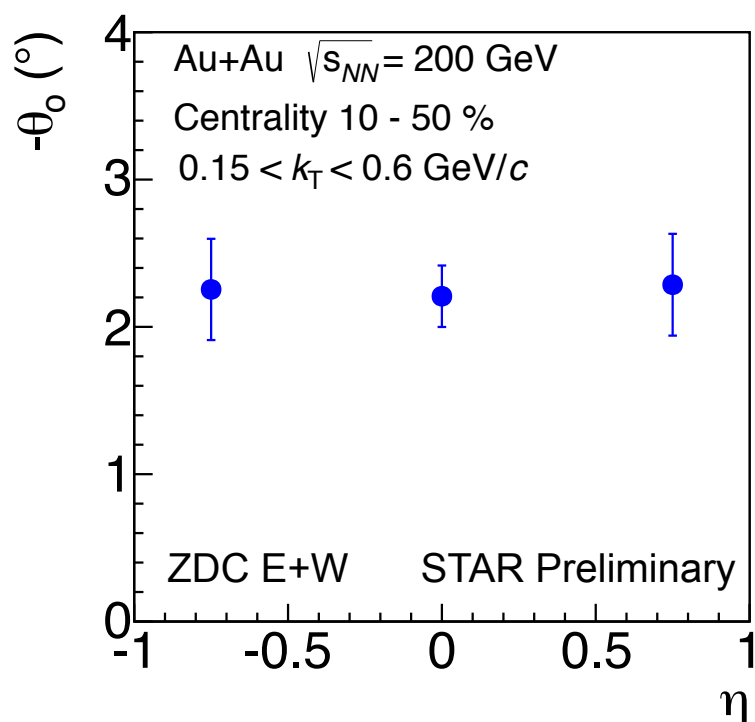
- θ_s purely corresponds to geometrical tilt (only side and long info. used)
- θ_o is that R_{ol,1} is used instead of R_{sl,1}
- Centrality dependence is very weak or absent
- Tilt angle shows similar trend to that of centrality dependence of v₁ slope



η dependence of tilt angle in Au+Au



• EP resolution correction is not applied

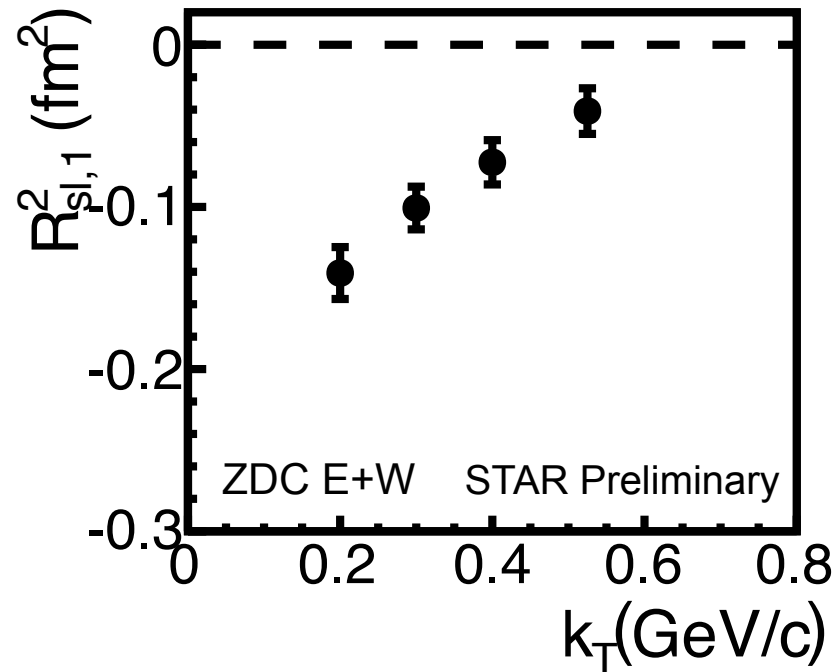
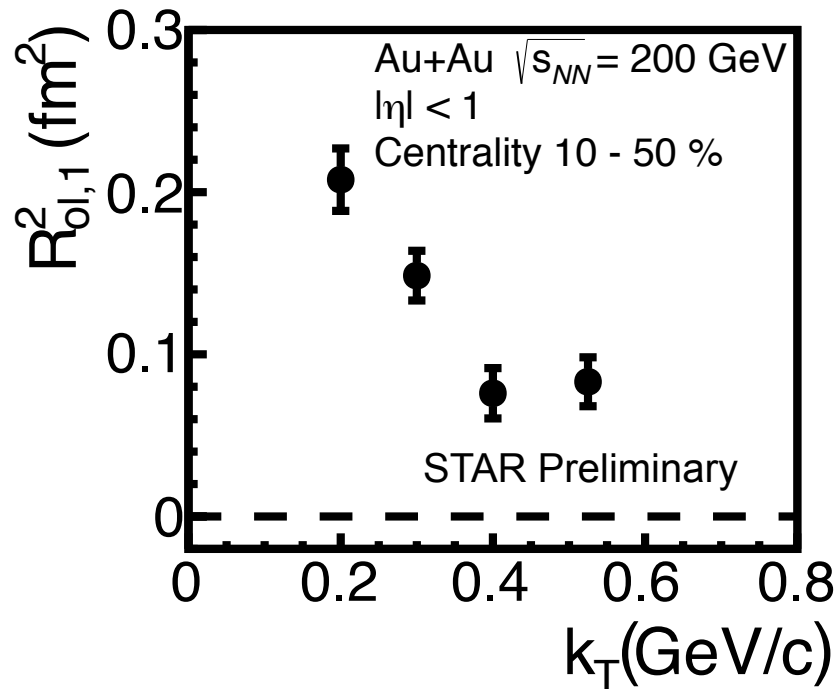


- The average R_{0l} value shifts when going away from center-of-mass rapidity
- The oscillation amplitude does not have significant dependence on η
- Same tilt angle can be seen in all η region
- These results are consistent with the linear dv_1/dy slope at midrapidity

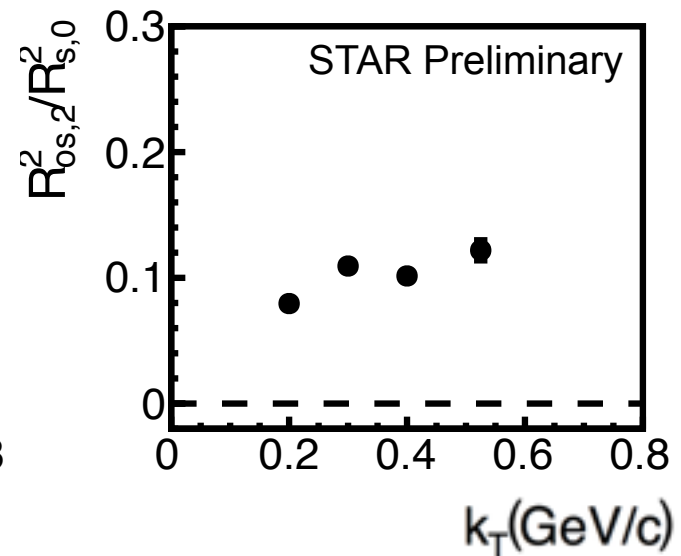
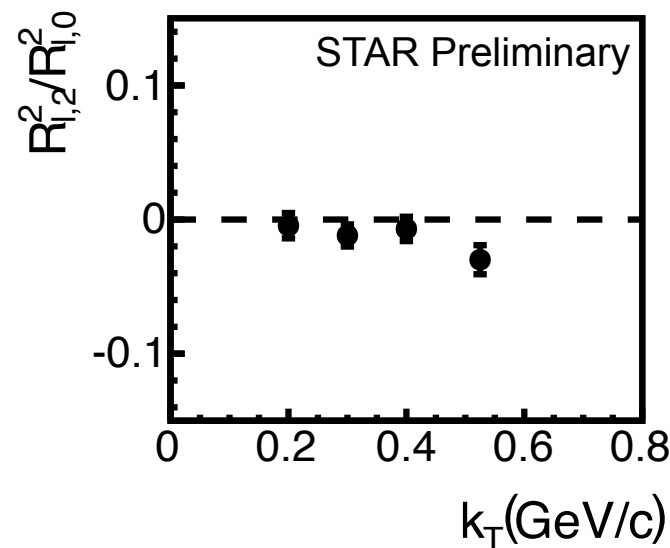
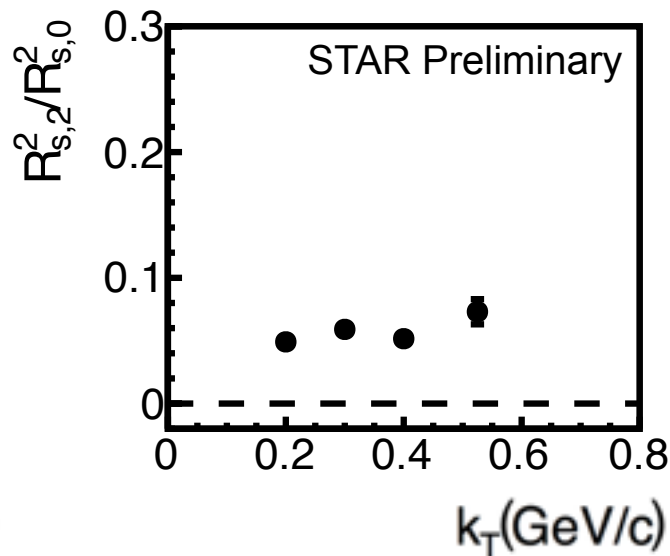
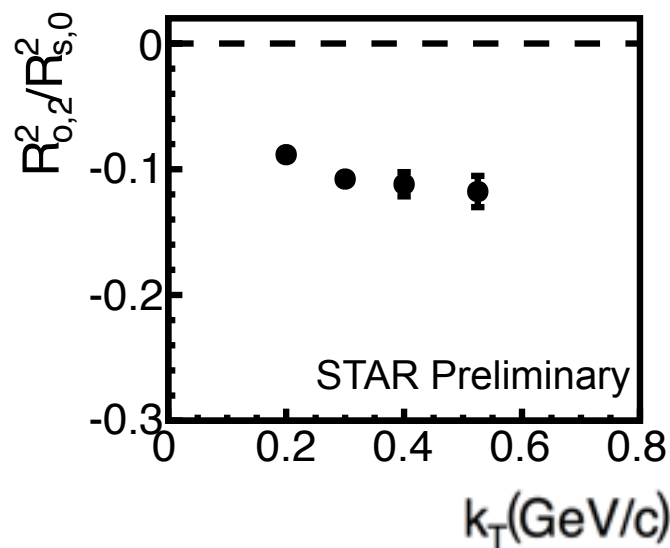


k_T dependence of HBT radii

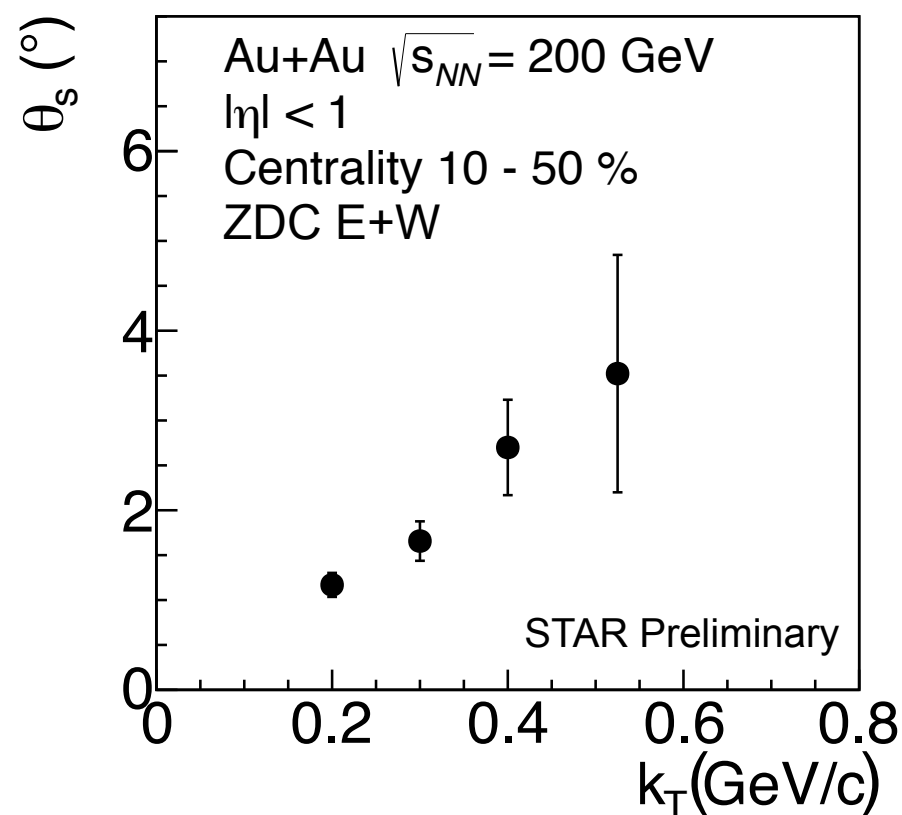
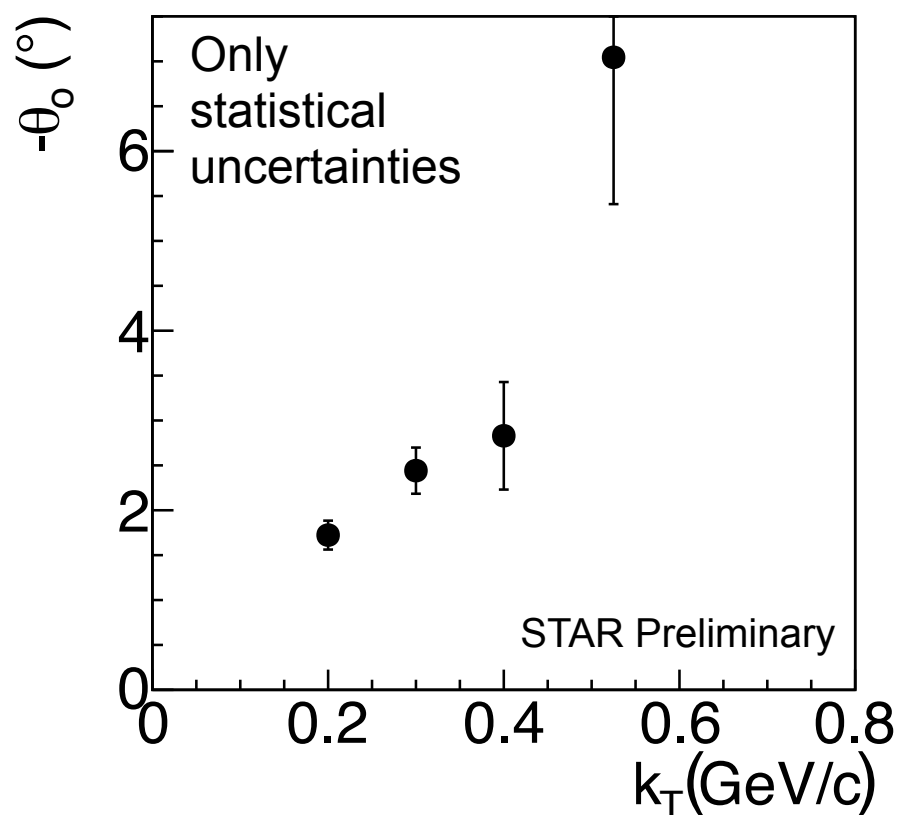
- The 1st-order oscillations



- The 2nd-order oscillations relative to the average radii



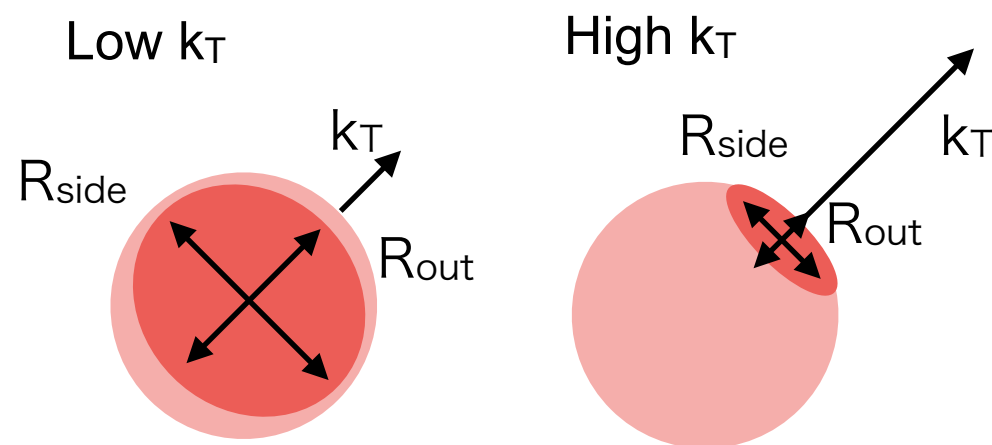
- The 1st-order oscillation magnitude $R_{s,1}$ $R_{o,1}$ seems to decrease with increasing k_T**
 -> The same trend as the centrality dependence
- The 2nd-order oscillations $R_{o,2}/R_{s,0}$, $R_{s,2}/R_{s,0}$, $R_{os,2}/R_{s,0}$ have weak k_T dependence compared to the centrality dependence**
 -> It means final eccentricity (ϵ_{final}) shows very weak dependence on k_T (in the measured k_T range)



Tilt angle

$$\theta_s = \frac{1}{2} \tan^{-1} \left(\frac{-4R_{sl,1}^2}{R_{l,0}^2 - R_{s,0}^2 + 2R_{s,2}^2} \right)$$

$$\theta_o = \frac{1}{2} \tan^{-1} \left(\frac{-4R_{ol,1}^2}{R_{l,0}^2 - R_{s,0}^2 + 2R_{s,2}^2} \right)$$



- Unlike centrality dependence, tilt angle seems to increase with k_T
- As the k_T increases, HBT radii decrease because of collective radial flow
 -> $(R_{l,0}^2 - R_{s,0}^2 + 2R_{s,2}^2)$ decreases faster than $R_{sl,1}$, contributing to an increase in the θ_s



- **Azimuthal-angle dependence of HBT radii w.r.t. Ψ_1**
 - ✓ The 1st-order oscillations of $R_{0|}$ and $R_{s|}$ have been measured in both Au+Au and Cu+Au collisions at 200 GeV

Final eccentricity (Au+Au 200 GeV)

- ✓ Final eccentricity w.r.t. Ψ_1^{ZDC} is consistent with that measured by Ψ_2^{TPC}
- ✓ Final eccentricity shows a centrality dependence and weakly depends on k_T

Tilt angle (Au+Au 200 GeV)

- ✓ Centrality dependence of tilt angle is very weak or absent and tilt angle seems to increase with increasing k_T
- ✓ Tilt angle seems to be η -independent within the TPC acceptance ($|\eta| < 1$)

Outlook

- Estimate systematic uncertainties
- Examine beam-energy dependence in BES-II with high statistics and good event plane resolution due to the installation of Event Plane Detector (EPD)

Back up

Au+Au 200 GeV

Run11 minimum bias

- Events ~ 430 M

Event selection

- $|v_z| < 25$ cm
- $|v_r| < 2$ cm
- $|v_z - v_z^{vpd}| < 3$ cm

Track selection

- $0.15 < p_T < 0.8$ GeV/c
- $|\eta| < 1$
- nHitsFit ≥ 15
- nHitsFit/nHitsPoss ≥ 0.52
- DCA < 3 cm

PID

- Tof Matched track
 - for $0.15 < p < 0.3$ GeV/c
 $m^2_\pi \pm 2\sigma, |n\sigma_\pi| < 3$
 - for $0.3 < p < 2.8$ GeV
 $m^2_\pi \pm 2\sigma, \text{veto } m^2_k \pm 2\sigma, |n\sigma_\pi| < 3$
- TPC only
 - for $0.15 < p < 0.5$ GeV/c
 $|n\sigma_\pi| < 2$
 - for $0.5 < p < 0.7$ GeV/c
 $|n\sigma_\pi| < 2, |n\sigma_k| > 2$

Cu+Au 200 GeV

Run12 minimum bias

- Events: ~ 45 M

Event Selection

- $|v_z| < 30$ cm
- $|v_r| < 2$ cm
- $|v_z - v_z^{vpd}| < 3$ cm

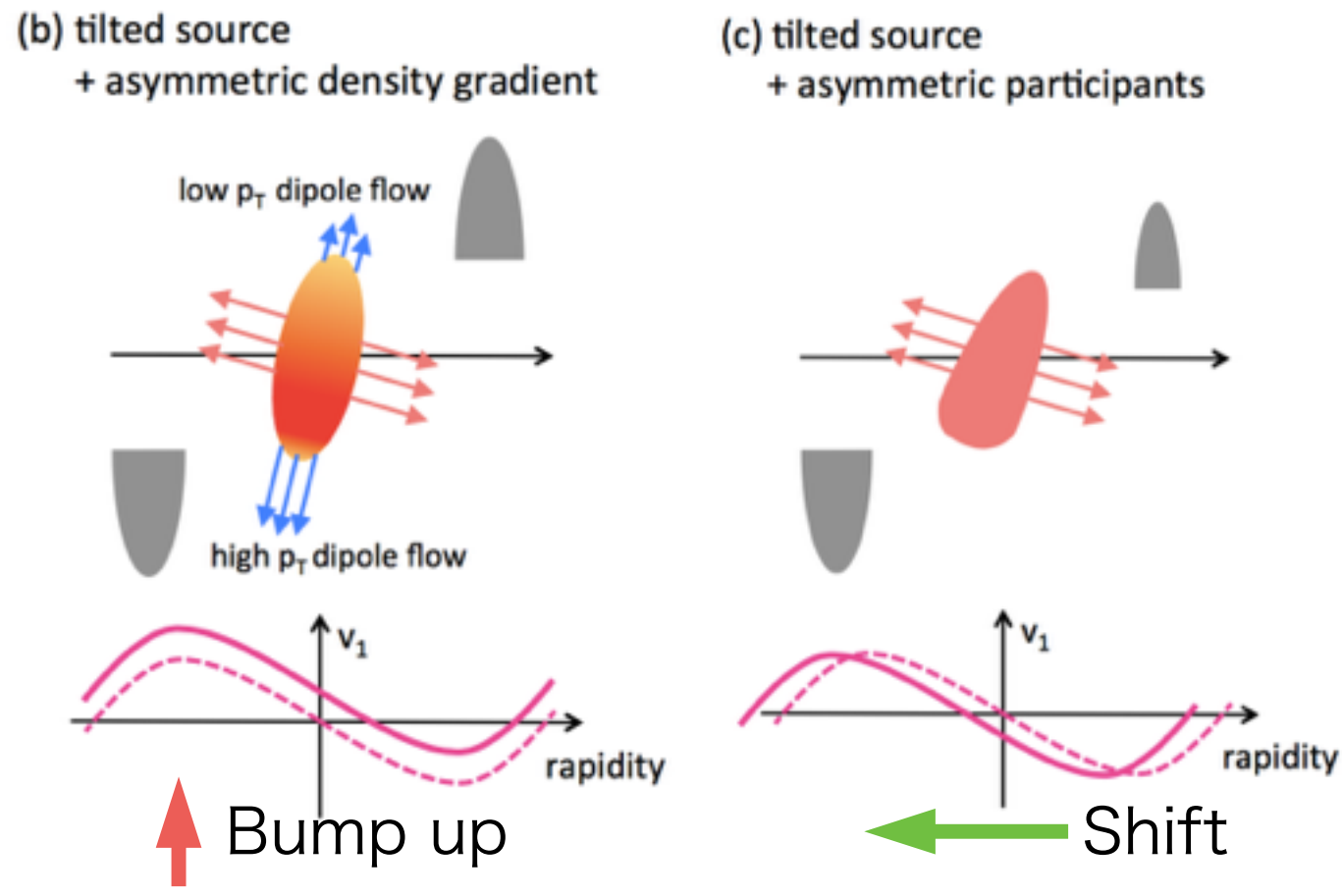
Track selection

- $0.15 < Pt < 0.8$ GeV/c
- $|\eta| < 1$
- nHitsFit ≥ 15
- nHitsdEdx ≥ 10
- nHitsFit/nHitsPoss ≥ 0.52
- DCA < 3 cm

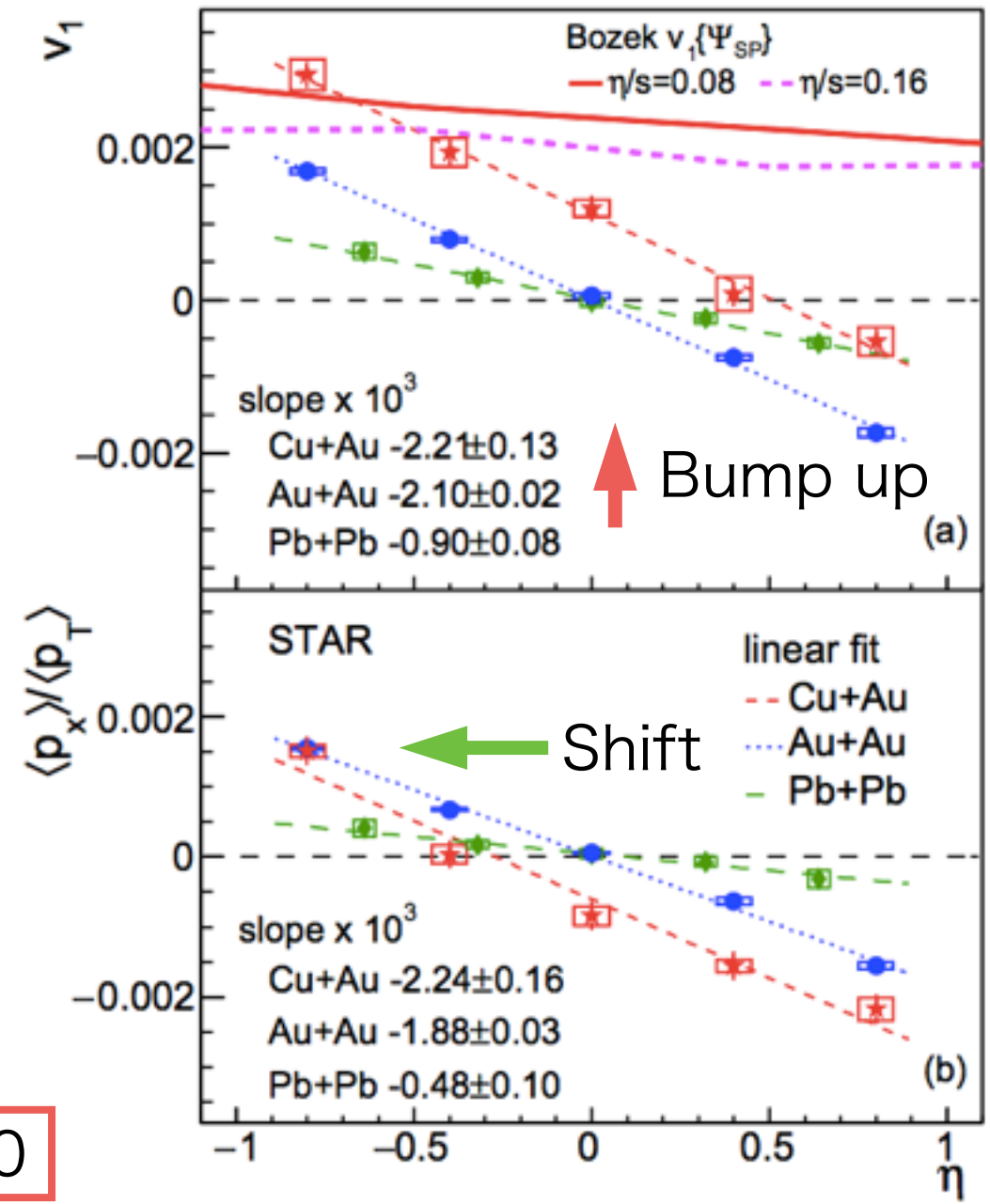
PID

- Tof Matched track
 - for $0.15 < p < 0.3$ GeV/c
 $m^2_\pi \pm 2\sigma, |n\sigma_\pi| < 3$
 - for $0.3 < p < 2.8$ GeV
 $m^2_\pi \pm 2\sigma, \text{veto } m^2_k \pm 2\sigma, |n\sigma_\pi| < 3$
- TPC only
 - for $0.15 < p < 0.5$ GeV/c
 $|n\sigma_\pi| < 2$
 - for $0.5 < p < 0.7$ GeV/c
 $|n\sigma_\pi| < 2, |n\sigma_k| > 2$

STAR Collaboration, Phys. Rev. C 98 (2018) 14915



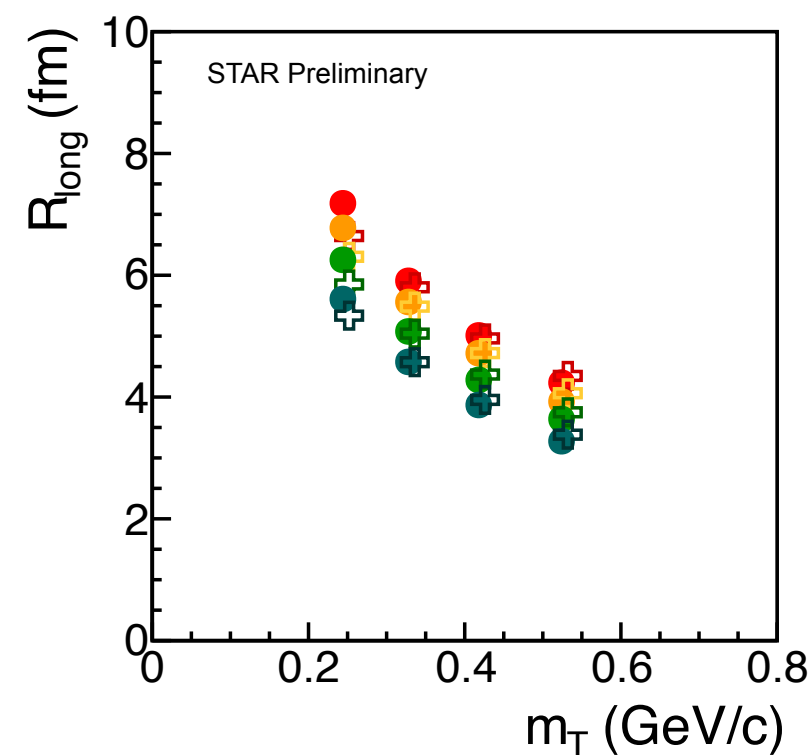
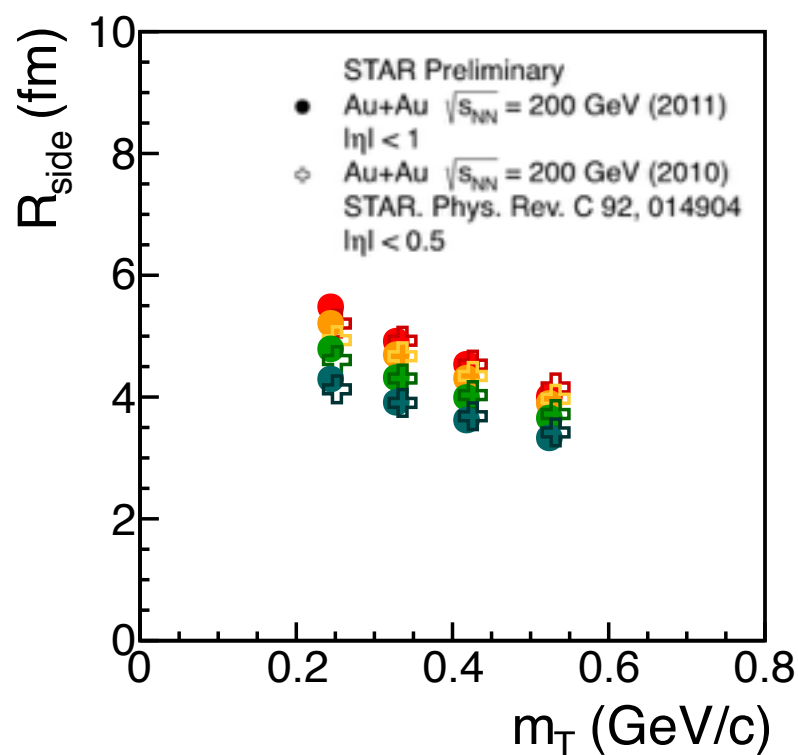
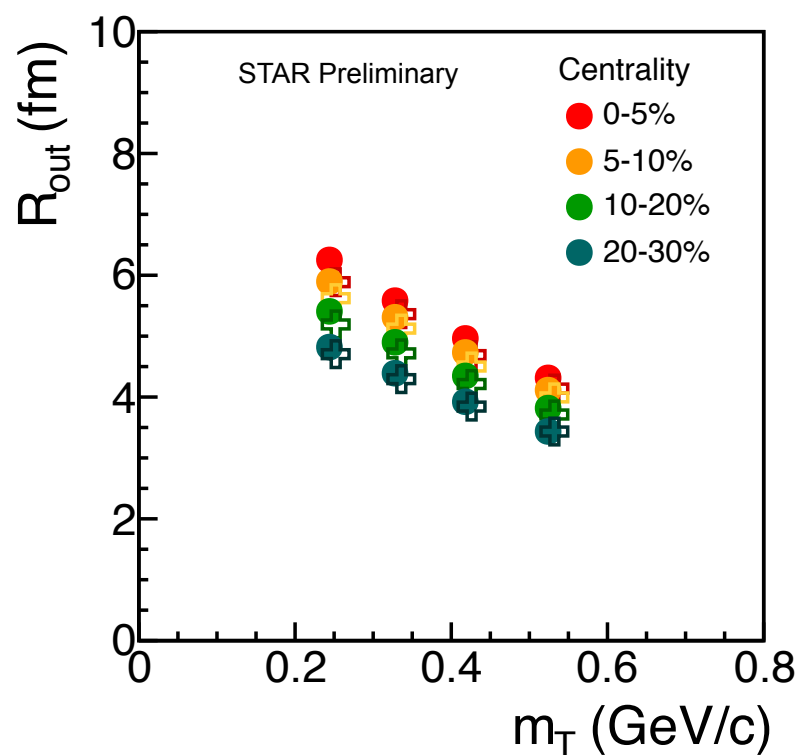
Note: $\langle p_x \rangle$ contribution from dipole flow ~ 0



- ✓ Cu+Au has asymmetric density gradient and it causes “dipole flow”.
 -> It bump up directed flow signals. (Fig. (b))
- ✓ In addition, Cu+Au collisions have a different number of participants between forward and backward directions.
 -> It shifts directed flow to the center-of-mass rapidity (Fig.(c))



HBT radii in Au+Au consistency check



✓ Average radii are consistent within systematic uncertainties

Source	R_{out}	R_{side}	R_{long}	ϵ_F
Coulomb	4%	3%	4%	0.004
Fit Range	5%	5%	5%	0.002
FMH	7%	3%	3%	0.003
Total	9.5%	6.5%	7%	0.005

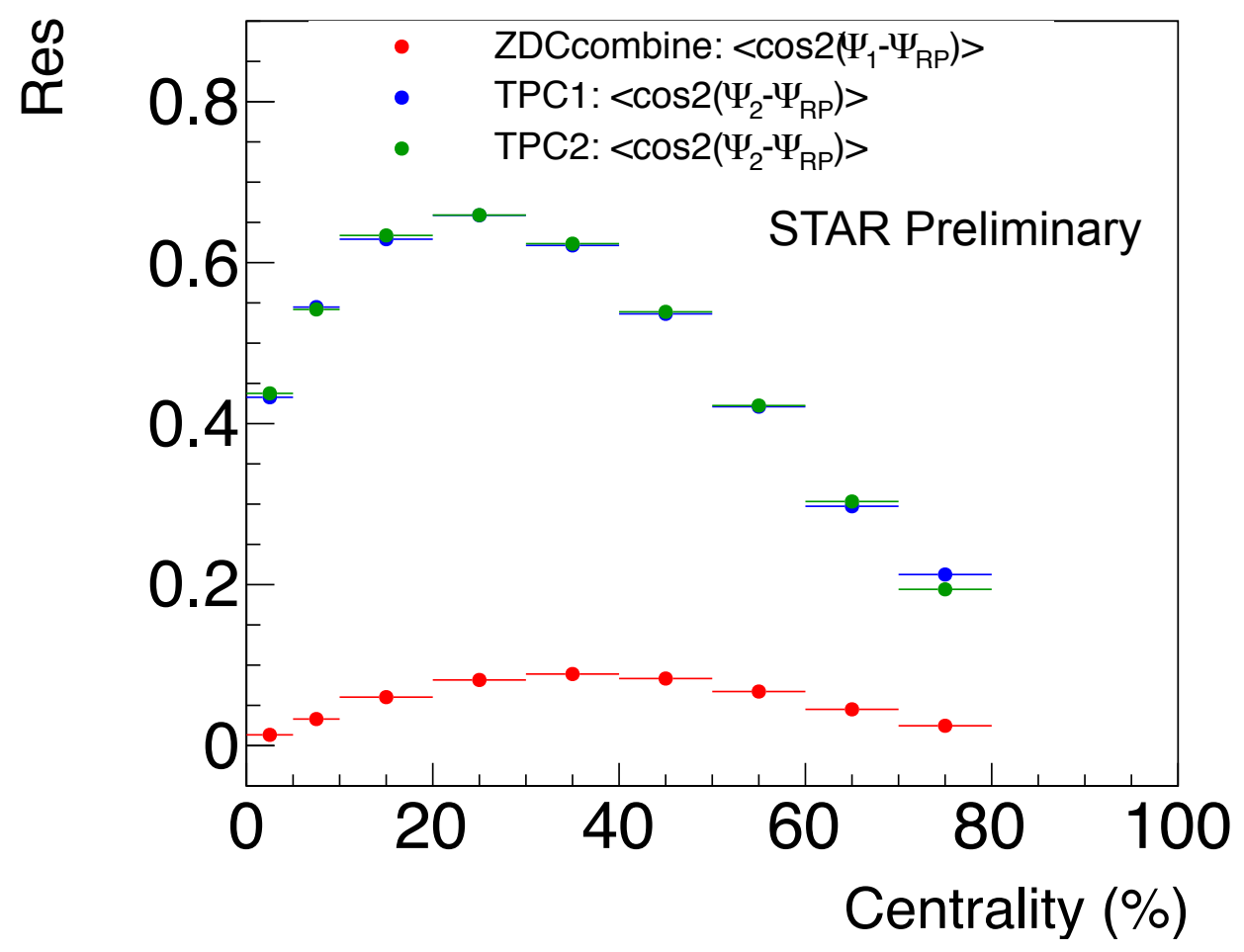
Systematic errors of average radii in
STAR Collaboration, Phys. Rev. C 92 (2015) 014904



EP resolution

- Au+Au 200 GeV

- $\langle \cos 2(\Psi_1 - \Psi_{RP}) \rangle$: 3 subevent method



There is a choice for EP resolution correction

- $\langle \cos(\Psi_1 - \Psi_{RP}) \rangle$ 2 subevent or 3 subevent method
- $\langle \cos 2(\Psi_1 - \Psi_{RP}) \rangle$ 2 subevent or 3 subevent method

S_{11} : source variance in x direction

S_{33} : source variance in z direction

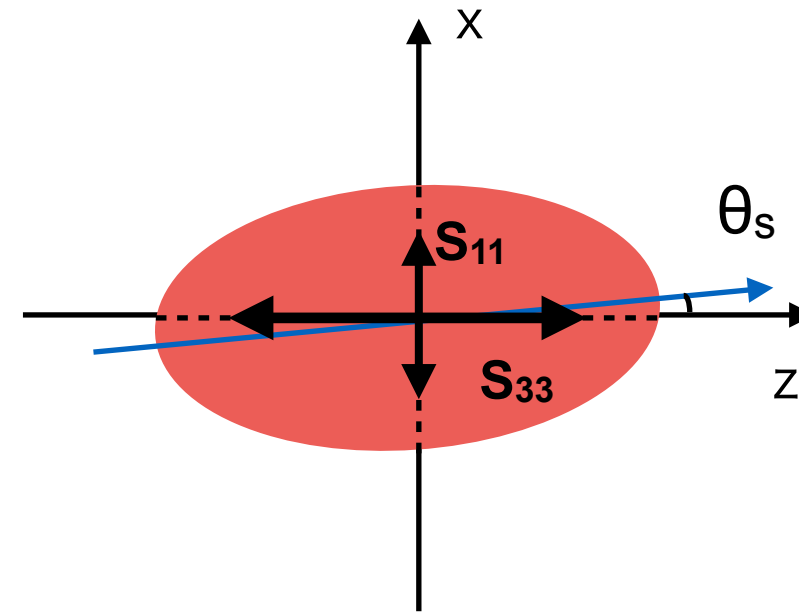
S_{13} : x-z covariance

$$S' = R_y^\dagger(\theta_s) \cdot S \cdot R_y(\theta_s)$$

$S_{\mu\nu}$: Spatial correlation tensor

$R_y(\theta_s)$: Rotation matrix

$$\theta_s = \frac{1}{2} \tan^{-1} \left(\frac{2S_{13}}{S_{33} - S_{11}} \right)$$



Rotating the spatial correlation tensor $S_{\mu\nu}$ by θ_s yields a purely diagonal tensor S'

$$R_{out}^2(\phi) = \frac{1}{2}(S_{11} + S_{22}) - \frac{1}{2}(S_{22} - S_{11})\cos(2\phi) + \beta_T^2 S_{00} \quad R_{os}^2(\phi) = \frac{1}{2}(S_{22} - S_{11})\sin(2\phi)$$

$$R_{side}^2(\phi) = \frac{1}{2}(S_{11} + S_{22}) + \frac{1}{2}(S_{22} - S_{11})\cos(2\phi) \quad R_{ol}^2(\phi) = S_{13}\cos(\phi)$$

$$R_{long}^2(\phi) = S_{33} + \beta_l^2 S_{00} \quad R_{sl}^2(\phi) = -S_{13}\sin(\phi)$$

Express in out-side-long coordinate

$$\theta_s = \frac{1}{2} \tan^{-1} \left(\frac{-4R_{sl,1}^2}{R_{l,0}^2 - R_{s,0}^2 + 2R_{s,2}^2} \right)$$